Brigham Young University
BYU ScholarsArchive

All Theses and Dissertations

2017-06-01

Enzyme Encapsulation, Biosensing Endocrine Disrupting Chemicals, and Bio-therapeutic Expression Platforms Using Cell-Free Protein Synthesis

Seung Ook Yang
Brigham Young University

Follow this and additional works at: https://scholarsarchive.byu.edu/etd

 Part of the Biochemistry Commons

BYU ScholarsArchive Citation

Yang, Seung Ook, "Enzyme Encapsulation, Biosensing Endocrine Disrupting Chemicals, and Bio-therapeutic Expression Platforms Using Cell-Free Protein Synthesis" (2017). *All Theses and Dissertations*. 6885.
https://scholarsarchive.byu.edu/etd/6885

This Dissertation is brought to you for free and open access by BYU ScholarsArchive. It has been accepted for inclusion in All Theses and Dissertations by an authorized administrator of BYU ScholarsArchive. For more information, please contact scholarsarchive@byu.edu, ellen_amatangelo@byu.edu.

Enzyme Encapsulation, Biosensing Endocrine Disrupting Chemicals, and Bio-Therapeutic Expression Platforms Using Cell-Free Protein Synthesis

Seung Ook Yang

A dissertation submitted to the faculty of
Brigham Young University
in partial fulfillment of the requirements for the degree of

Doctor of Philosophy

Bradley C. Bundy, Chair
Gregory F. Burton
Randy S. Lewis
John C. Price
David J. Michaelis

Department of Chemistry and Biochemistry

Brigham Young University

Copyright © 2017 Seung Ook Yang

All Rights Reserved

ABSTRACT

Enzyme Encapsulation, Biosensing Endocrine Disrupting Chemicals, and Bio-Therapeutic Expression Platforms Using Cell-Free Protein Synthesis

Seung Ook Yang
Department of Chemistry and Biochemistry, BYU
Doctor of Philosophy

Cell-free protein synthesis (CFPS) is a powerful protein expression platform where protein synthesis machinery is borrowed from living organisms. Target proteins are synthesized in a reaction tube together with cell extract, amino acids, energy source, and DNA. This reaction is versatile, and dynamic optimizations of the reaction conditions can be performed. The "open" nature of CFPS makes it a compelling candidate for many technologies and applications.

This dissertation reports new and innovative applications of CFPS including 1) enzyme encapsulation in a virus-like particle, 2) detection of endocrine disrupting chemicals in the presence of blood and urine, and 3) expression of a multi-disulfide bond therapeutic protein.

Two major limitations of enzymes are their instability and recycling difficulty. To overcome these limitations, we report the first enzyme encapsulation in the CFPS by immobilizing in a virus-like particle using an RNA aptamer. This technique allows simple and fast enzyme production and encapsulation

We demonstrate, for the first time, the Rapid Adaptable Portable In vitro Detection biosensor platform (RAPID) for detecting endocrine disrupting chemicals (EDCs) in human blood and urine samples. Current living cell-based assays can take a week to detect EDCs, but RAPID requires only 2 hours. It utilizes the versatile nature of CFPS for biosensor protein complex production and EDC detection.

Biotherapeutic protein expression in *E. coli* suffers from inclusion body formation, insolubility, and mis-folding. Since CFPS is not restricted by a cell wall, dynamic optimization can take place during the protein synthesis process. We report the first expression of full-length tissue plasminogen activator (tPA) using CFPS.

These research works demonstrate the powerful and versatile nature of the CFPS.

Keywords: Seung Ook Yang, cell-free protein synthesis, enzyme encapsulation, enzyme immobilization, endocrine disrupting chemicals, RAPID, blood, urine, therapeutic protein, tissue plasminogen activator

ACKNOWLEDGEMENTS

First and foremost, I would like to thank my advisor, Professor Brad Bundy, for the guidance and encouragement he has shared with me during my time in the graduate program. I would like to thank the Bundy lab members, Mark, Amin, Andrew, Matt, Kristen, and Porter, for all the support extended, great memories, and learning experiences. I want to thank both the Department of Chemical Engineering and the Department of Chemistry and Biochemistry at BYU, particularly the members of my committee members (Dr. Burton, Dr. Lewis, Dr. Michaelis, and Dr. Price) for their time and willingness to mentor me. I'd like to extend my gratitude to David Eddinton for the kind blood donation, Michael Standing for the Tecnai-12 TEM training, Paul Minson for providing VLP images with his Tecnai-20 TEM, and Dr. Dixon Woodbury for DLS analysis.

I would finally like to thank my family and friends for their love and sacrifice. Words cannot fully express my gratitude for their encouragement, advice, and love they have given me over the years. I would not be where I am today without them.

TABLE OF CONTENTS

LIST OF TABLES

LIST OF FIGURES

1 INTRODUCTION

1.1 Background

Cell-free protein synthesis (CFPS) is the production of proteins using biological protein synthesis machinery from living cells but without the use of the living cells. Components of the CFPS reaction consist of cell extract, energy source, salts, amino acids, and desired DNA. CFPS has many advantages over *in vivo* protein synthesis: 1) Cell extract preparation together with protein synthesis takes only 2 days while *in vivo* expression may take 1-2 weeks.[1-2] 2) CFPS is not restricted by the cell wall. This environment allows direct accessibility, optimization, and dynamic control on protein synthesis.[3-4] 3) Toxicity is not a concern in the CFPS. Some proteins are toxic to the host cells,[5-6] whereas CFPS can produce toxic proteins without concerns of cell death.[3] 4) Unnatural amino acids can be introduced while synthesizing proteins.[7-9] Both the modified aminoacyl tRNA synthetase and unnatural amino acids can be incorporated in CFPS reactions for many applications. 5) It enables post translational modifications (PTM). CFPS reactions possess PTM abilities, such as glycosylation and phosphorylation.[10-11]

Today, common extracts are prepared from Escherichia coli (*E. coli*), rabbit reticulocytes, wheat germ, and insect cells.[1] Among those, cell lysate from the *E. coli* is the most commonly used extract for its cost-effective, robust, less time/labor intensive, and high expression level nature to synthesize proteins. CFPS based on *E. coli* cell extracts have shown potential to express difficult-to-synthesize proteins, such as membrane proteins,[12-13] multi-disulfide bond proteins,[4, 14]

proteins with post-translational modification,[11] cytotoxic proteins,[3] metallic holoenzymes,[15-16] and virus-like particles.[17-18] Also, the robust nature of CFPS allows changes in reaction temperature,[4, 11] time,[11] pH,[19] and redox potential.[4, 14] Many industries favor these advantages and the versatile nature of the CFPS.

Our lab has been leveraging on the advantages of the CFPS to harness innovative industrial technologies, with a couple of them being introduced here. We expressed cytotoxic cancer biotherapeutic (onconase) in CFPS[3] and tested the robust nature of the CFPS. Onconase is a ribonuclease that is effective against many types of cancers.[20-22] Expression and purification of onconase from oocytes of the Northern Leopard Frog is time and labor intensive.[20, 23-24] Previous attempts to express the enzyme using E. coli cells resulted in the formation of inclusion bodies. In our CFPS reaction, we simply added an additional amount of tRNAs to the onconase synthesis reaction at every 15 or 30 min. The onconase production level was 56-fold greater than that of conventional CFPS reaction with over 95% solubility. Lyophilized CFPS was used in onconase production for potential rapid, mobile, and on-demand therapeutics synthesis purposes. The lyophilized CFPS performed as well as or better than the standard CFPS reaction with the added tRNAs.

Site-specific covalent immobilization was achieved to enhance enzyme stability. Immobilization allows enzymes to overcome their limitations like being unable to recover and be reused,[25] resulting in a significant decrease in the cost of enzymes used. T4 lysozyme was used as a model enzyme. Amber codon usage enabled the incorporation of an unnatural amino acid (p-propargyloxyphenylalanine, pPa) in a site-specific manner. Covalent immobilization of the pPa incorporated T4 lysozyme to the superparamagnetic beads was done via a click reaction between the azide group of the bead and the 1, 3-dipolarophiles of the pPa incorporated T4 lysozyme.

Immobilized T4 lysozyme showed enhanced stability against freeze-thaw and post-urea incubation tests.

We seek to expand areas of research using CFPS. Here, we report new industrial applications of CFPS.

1.2 Archive of Research Projects

Although demands for the powerful and robust nature of *in vitro* protein production system are rising,[26] there is still high potential in the unexplored CFPS utilizations and technologies. In this work, we aim to explore promising areas of CFPS and exploit its open and robust nature.

1.2.1 Simple Two-step in vitro Enzyme Encapsulation using CFPS

This chapter introduces a new application of CFPS in target enzyme encapsulation. This is the first time CFPS system is utilized for target enzyme encapsulation. A simple two-step CFPS is required for this work.

1st Step: Optimization of Target Enzyme Production - *Candida antarctica* lipase B (CalB) possesses multi-disulfide bonds. Attempts to express CalB in conventional *in vivo E. coli* resulted in the formation of inclusion bodies and non-functional CalB. To enhance correct folding and the solubility of functional CalB, cell extract containing overexpressed GroEL/ES and optimized glutathione buffer mix were added to the CalB's CFPS reaction.

2nd Step: Expression of Capsid Protein with CalB from the Step 1 – Bacteriophage Qβ capsid was expressed in the 2nd CFPS. The overexpressed GroEL/ES and the glutathione buffer mix was not needed; instead, crude CalB solution from the step 1 and an RNA aptamer were added to the 2nd CFPS. 5'end and 3' end of the aptamer had affinities towards the CalB and

capsid, respectively. During the expression and assembly of the capsid, the enzyme is guided by the aptamer for encapsulation. The nickel affinity purified capsid contained functional CalB, and the encapsulated enzyme showed stability against both temperature and protease inactivation.

1.2.2 Cell-free Protein Synthesis Approach to Biosensing hERβ-specific Endocrine Disruptors

This chapter discusses the open and robust nature of CFPS that allows the detection of endocrine disrupting chemicals. CFPS expressed a nuclear hormone receptor protein complex (hERβ) in the presence of varying concentrations of ligands with no decrease in its activity. Human blood and urine samples decreased CFPS reaction activity significantly. The addition of RNAse inhibitor to the CFPS regained its activity. Limit of detection, EC50, z' factor, and signal to noise/background were calculated and reported.

1.2.3 Multi-disulfide Bond Protein Expression in CFPS

This chapter introduces the first attempt to express the full-length tissue-plasminogen activator (tPA) in CFPS. tPA possesses 17 disulfide bonds and is difficult to express the functional protein. Truncated tPA or the protease domain alone have been expressed in the CFPS reaction. Many attempts to produce functional tPA in *E. coli* suffer from inclusion body formation and mis-folding. We introduced disulfide bond protein C (DsbC) to our CFPS reaction of tPA in addition to the overexpressed GroEL/ES and the glutathione buffer mix. DsbC is believed to help correct disulfide bonds of the tPA. Nickel affinity column purified the non-glycosylated tPA, and the pure enzyme possessed minor activity.

2 SIMPLE IN VITRO TWO-STEP ENZYME ENCAPSULATION IN CELL-FREE PROTEIN SYNTHESIS

2.1 Introduction

Here, we demonstrate a simple two-step *in vitro* enzyme encapsulation in the capsid of bacteriophage Qβ using cell-free protein synthesis (CFPS) with *Candida antarctica* lipase B (CalB) as a guest enzyme (Figure 2-1). The first step requires the cell-free synthesis of the target enzyme. The expressed enzymes are directly transferred to the second cell-free synthesis, VLP expression. Purification of the target enzyme is not needed, and the encapsulation is target enzyme specific

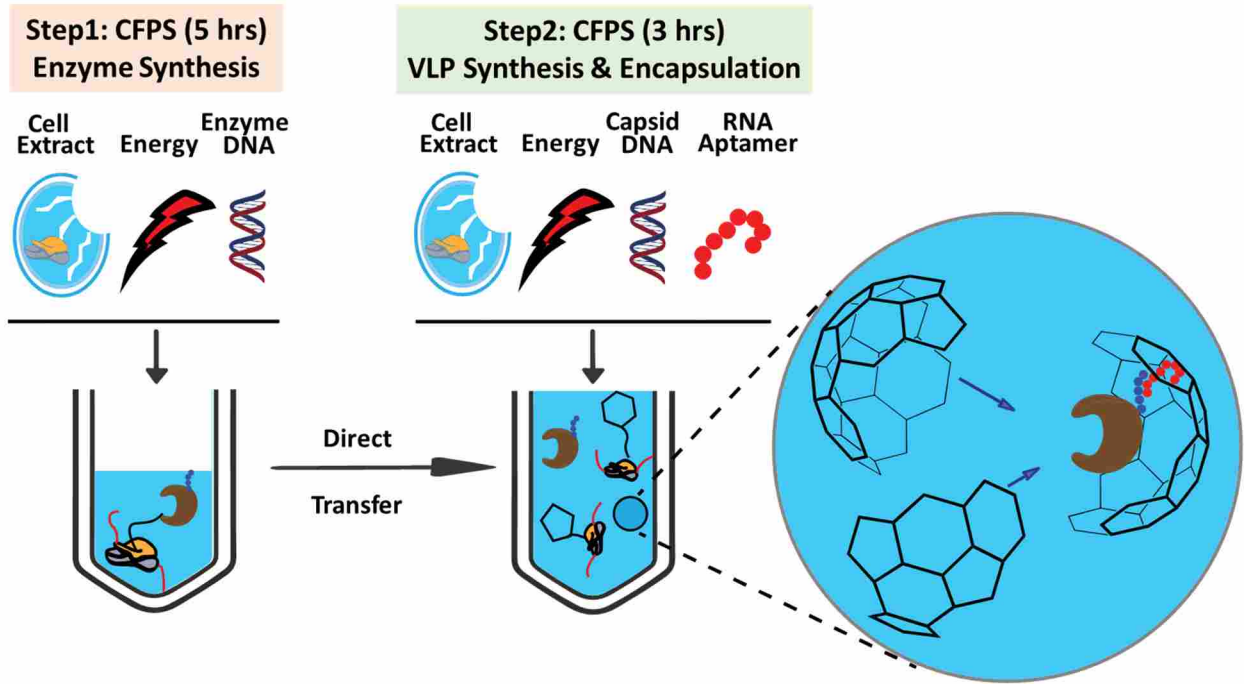

Figure 2-1 Enzyme Encapsulation Using Two-step Cell-free Protein Synthesis CFPS-based enzyme encapsulation targets enzyme specific reaction via RNA aptamer. 5'-and 3'-end of the aptamer sequences target enzymes with a specific peptide tag and the interior surface of the VLP, respectively.

due to RNA aptamer. We also demonstrate a controlled enzyme encapsulation efficiency by simply adding a varying amount of CalB to the Qβ virus-like particle (VLP)'s CFPS reaction. CFPS is a robust protein expression system and is not confined within the cell wall. Guest molecules can be easily introduced[3-4] to achieve dynamic optimization in the CFPS.[27-28] To facilitate functional CalB encapsulation, the optimized CalB product from the CFPS and an RNA aptamer are directly added to the CFPS reaction of the Qβ capsid. Encapsulated CalB possesses similar kinetic parameters to the free CalB, but shows higher stability against high temperatures and a protease.

Enzymes can catalyze a wide variety of biochemical reactions and are used in many different industries, such as biofuel,[29] detergent,[30] brewing,[31] dairy,[32] food processing,[33] molecular biology,[34] paper,[35] and personal care industries.[36] Although they are rapid, specific, biodegradable, and cost/energy efficient, they are unstable to small changes in temperature and pH. Expensive enzyme production and short longevity are additional concerns

Scientists have been developing ways to overcome those limitations, such as adsorption,[37-38] covalent bonding,[7-8] entrapment,[39-41] cross linking,[42-43] and encapsulation.[6, 44-46] Out of all those methods, enzyme encapsulation is particularly interesting for many reasons: 1) multiple enzymes can be introduced in a single step,[47] 2) encapsulated enzymes are stable,[46, 48] 3) native structure (activity) of enzyme is maintained,[44-48] and 4) it is a cost effective method.[49]

Nature has been adopting target enzyme encapsulation in microcompartments. Bacterial microcompartments (BMCs) encapsulate enzymes and other proteins in their protein shells. Their diameter varies between 40 and 200 nm.[50-53] The protein shell serves as a selective permeable membrane.[54-55] Enzymes and proteins found in the BMCs carry out specific chemical, often sequential, reactions.[56] Despite the advantages, the capsid assembly can be complicated as it requires multiple protein shells.[57] Also, only a few capsid-guest enzyme interactions have been

identified.[58, 59]

Viruses evolve to encapsulate specific guest molecules, such as nucleic acids (DNA and RNA) and enzymes. Their genetic materials are protected by capsids. Nanotechnologists are interested in mimicking BMCs using virus-like particles (VLP) due to its well-known specific interaction between its protein shell and guest molecules for selective encapsulation,[46] self-assembly of capsid,[46, 60] confined space for chemical reaction,[45-47] and guest molecule protection ability.[46]

To date, three VLPs have been extensively used for target enzyme encapsulation, including Cowpea chlorotic mottle virus (CCMV),[44] bacteriophage Qβ,[46] and bacteriophage P22.[45, 47] Each VLP utilizes a unique method to encapsulate guest enzymes. CCMV can exist in an assembled (pH 5) or a disassembled state (pH 7.5).[61-63] Minten and colleagues prepared two coiled-coil motifs for target enzyme encapsulation, each having seven amino acids repeat. The first and penultimate residues of the repeat were charged molecules with either all glutamate (E-coil) or lysine (K-coil).[62] The K-coil is fused to the capsid and enzymes for the E-coil. The coiled-coil (*in vitro*) method utilizes heterodimer-forming coils attached to both guest enzyme and CCMV coat protein to link the two proteins (pH 7.5) prior to the capsid assembly (pH 5).[61-63]

Bacteriophage P22 utilizes scaffolding proteins for enzyme sequestration. Target enzymes were fused to the N-terminus of the scaffolding protein (SP), and the fusion protein was guided to the lumen of the P22 capsid during the capsid assembly via C-terminus of the SP.[45, 47]

RNA aptamer-guided enzyme encapsulation was done with bacteriophage Qβ capsid. Hairpin loop forming RNA sequence from the Qβ binds specifically to the interior surface of the Qβ capsid.[64-65] Fiedler and colleagues made an RNA aptamer by fusing an arginine rich (Rev) tag

binding sequence and the hairpin loop sequence to the 5'-end and 3'-end of the Qβ capsid template, respectively.[46] The RNA aptamer was transcribed during *in vivo* capsid translation. The Rev-tag fused guest enzymes were encapsulated via the RNA aptamer during *in vivo* protein expression and capsid assembly process.

We used the Qβ capsid for such nanotechnology because 1) it can be expressed in both *E. coli*[46] and cell-free protein synthesis (CFPS),[18] 2) the expressed Qβ can readily form a capsid consisting of 180 monomers (T = 3) with an average of 27 nm diameter,[66] 3) five-/three-fold axis[66] and large six-fold axis pores[46] of Qβ allow small molecules like substrates to penetrate through the capsid, 4) the Qβ capsid possesses binding specificity towards the RNA of the bacteriophage,[64-65] and 5) Qβ capsid is stabilized by disulfide bonds and is stable against high temperatures and acidic conditions.[67] In addition, P22 capsid is not stable against high temperatures.[45] Heating the capsid at 75˚C for 20 min could cause capsid expansion with large 10-nm holes at every five-fold vertices, and capsid subunits could be released from the assembly.[68-69] CCMV is unstable against pH. High pH at 7.5 and above will disassemble the capsid.[61-63] Purification of both the capsid and guest enzymes are crucial steps for enzyme encapsulation, which can be time consuming and labor intensive.

CFPS based *in vitro* enzyme encapsulation using Qβ capsid overcomes the major limitations that previous *in vivo* enzyme encapsulation possesses. CFPS can control the amount of guest enzymes introduced to the capsid assembly. Previous *in vivo* enzyme encapsulation using Qβ capsid could not control the amount of guest enzymes due to its co-production with the capsid.[46] Although varying amount of enzymes were encapsulated, encapsulation efficiency seemed to be complicated as it was affected by media components and magnesium concentration. Significant amounts of encapsulated enzymes, even when missing either RNA aptamer or Rev-tag,

indicates that the title “RNA-directed packaging of enzymes” is misleading. On the other hand, our CFPS-based enzyme encapsulation is solely affected by our RNA aptamer design. The arginine-rich peptide (Rev) tag targeting DNA sequence and the Qβ targeting sequence are fused to 5’- end and 3’-end of the Qβ DNA template, respectively. The aptamer is amplified using PCR. The RNA aptamer is transcribed by T7 RNA polymerase. Also, enzyme encapsulation efficiency in CFPS is controlled only by the amount of enzymes introduced. No significant enzyme encapsulation occurs in the absence of an RNA aptamer.

2.2 Results and Discussion

2.2.1 Simple Purification of Bacteriophage Qβ: Spin His-column

The conventional ways of purifying virus-like particles (VLPs) are by using either sucrose density gradient or size exclusion columns. While both methods are excellent in VLP

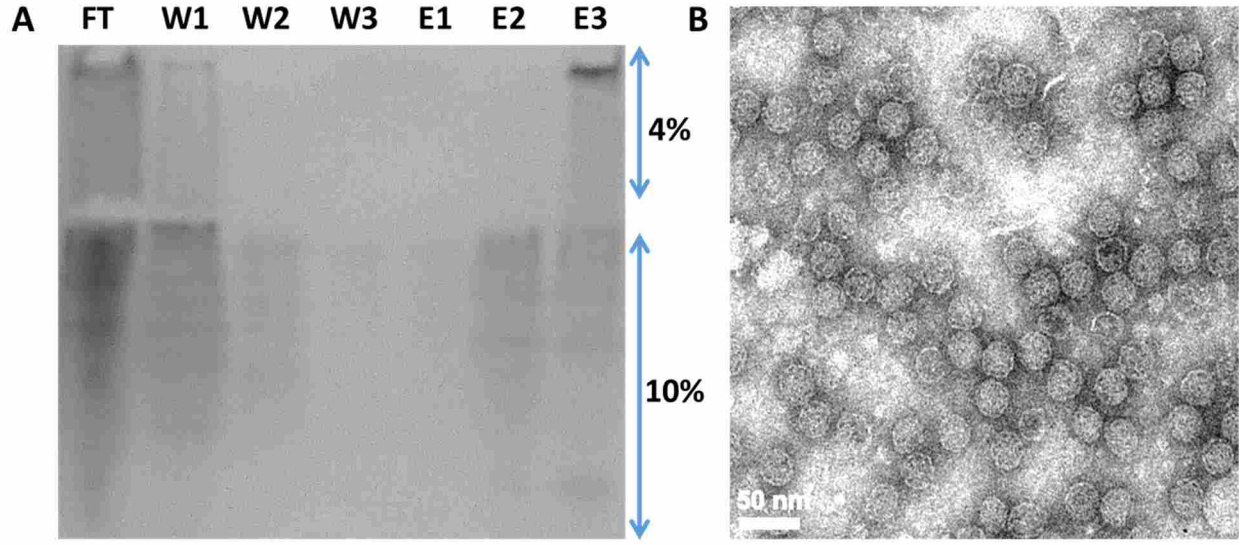

Figure 2-2 Simple Purification of Qβ VLP and TEM Image of the Pure VLP A six-Histidine tag fused VLP was purified by an increasing concentration of imidazole using a Spin-His column. Size and shape of the VLP was analyzed by TEM. **A** Each fraction of the Nickel column purification process was loaded on a Native gel. FT: flow through, W1: washing step 1, W2: washing step 2, W3: washing step 3, E1: elution with 40 mM imidazole, E2: elution with 100 mM imidazole, and E3: elution with 500 mM imidazole. **B** TEM image of the pure Qβ VLP. Spherical shaped VLP had a mean diameter of 30 nm.

Table 2-1 Details on Size, Activity, and Encapsulation Efficiency

	% Soluble Protein	Mean Diameter	Specific Activity (μmole/min/mg)	Average Number of Rev-CalB Encapsulation Per Amount of Rev-CalB Added
VLP	89.5%	33.3 ± 0.7 nm (DLS)	n/d	n/a
		30.2 ± 0.4 nm (TEM)		
Rev-CalB	93.8%	n/a	$4.3 \times 10^{-1} \pm 0.064$	n/a
Rev-CalB + VLP	84.4%	27.0 ± 2 nm (TEM)	$2.2 \times 10^{-1} \pm 0.022$	$6.5 \pm 2 \ / \ 1.7 \times 10^{4}$ ng
				$3.5 \pm 1 \ / \ 1.4 \times 10^{4}$ ng
				$1.0 \pm 0.7 \ / \ 8.4 \times 10^{3}$ ng

purification, they are time consuming, labor intensive, sensitive to vibration, jolt, and tilt. Here, Nickel affinity column purification of a six-Histidine tag fused Qβ purification is demonstrated. It is a simple and fast capsid purification by a spin His-column. The average concentration of the soluble capsid was 650 ng/μL from 500 μL reaction, and pure capsids showed greater than 76% recovery. Samples from the spin His-column were further analyzed using Native gel analysis as shown in Figure 2-2A. The first third of the gel is 4% acrylamide and the rest is 10%. As proteins migrate in the gel, unassembled capsid species will migrate to the interface of the 4% and 10% polyacrylamide. Fully assembled VLPs will remain on the top of the gel. The native PAGE results were in line with our hypothesis. The size and shape of pure capsids were measured with dynamic light scattering (DLS) and transmission electron microscope (TEM) as shown in Figure 2-2B and Table 2-1. Almost all pure-capsids were 33 nm diameter with DLS analysis. The TEM image showed circular and fully assembled VLPs with a mean diameter of 30 nm.

2.2.2 Rev-CalB Expression

Candida antarctica lipase B (CalB) is one of the most widely used lipases due to its region-/enantio selectivity,[4, 70] stability,[70] compatibility with organic solvents,[71] and wide variety of substrate selectivity.[71] CalB belongs to the α/β-hydrolase family[72] and possesses a catalytic triad, that consists of Ser-His-Asp.[73] There are 317 amino acids in the polypeptide chain with a molecular mass of about 33 kDa, and three disulfide bridges stabilize the conformation.[74]

Many eukaryotic microorganisms[75-77] have been used for the expression and protein engineering of the lipase.[78-80] There have been attempts to synthesize CalB in *E. coli* periplasm[71, 81] and cytoplasm.[82] However, such methods have disadvantages like low soluble lipase yield and inclusion body formation, the latter being a result of using temperatures higher than 20˚C in *E. coli* expression system.[83] In addition, CalB expression at a low temperature of 20˚C takes about two days to get a usable amount of soluble lipase.

To improve soluble yield of the recombinant lipase in the cell-free system, an *E. coli* strain that has overexpressed GroEL and GroES was prepared as described in the previous *in vitro* CalB expression.[4] A glutathione buffer (5 mM) was added to the CalB CFPS reaction at a fixed ratio between glutathione oxidized (GSSG) and reduced (GSH)[4] at 30˚C. More than 93% of the recombinant lipase was soluble, and the mean soluble yield was 306.8 ng/μL from a 70 uL reaction.

2.2.3 Two-Step Rev-CalB Encapsulation

To facilitate RNA aptamer-guided enzyme encapsulation, an arginine rich peptide (Rev) tag was fused to the N-terminus of the CalB. Rev-CalB (non-pure) CFPS reaction was directly transferred to the cell-free reaction of the Qβ capsid (step 2) along with an RNA aptamer. The

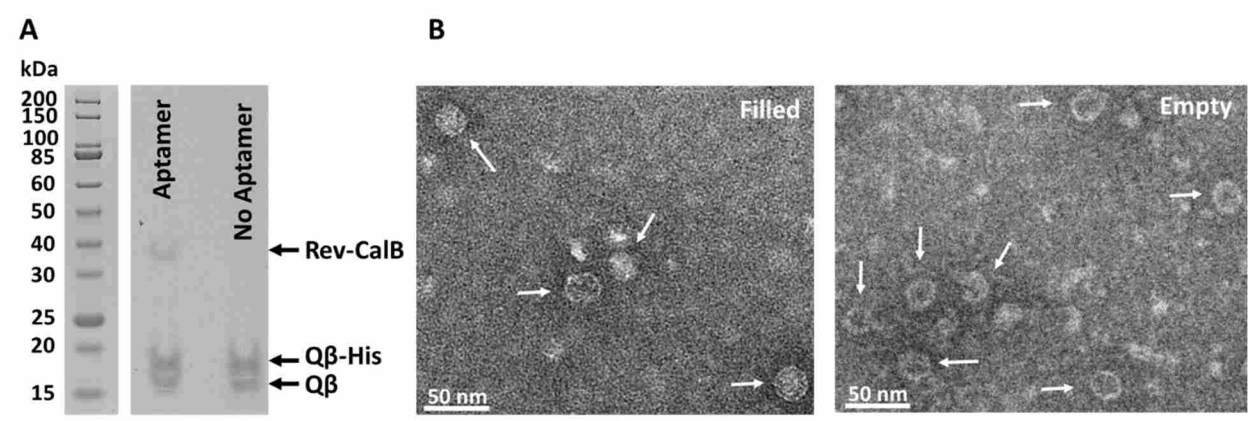

Figure 2-3 Filled Capsid vs Empty Capsid RNA aptamer played a major role in target enzyme encapsulation. **A** Autoradiogram analysis on the encapsulated enzyme and empty capsids. The target enzyme encapsulation was guided by the RNA aptamer as the radiolabeled Rev-CalB protein band appeared. **B** TEM image of the filled vs empty capsids. Negatively stained protein samples showed less stained inner capsids for the filled compared to the empty.

concentration of soluble capsid produced in the presence of Rev-CalB and RNA aptamer was 400 ng/μL in 160 μL CFPS reaction. The capsid production level decreased when Rev-CalB and RNA aptamer were introduced to the capsid CFPS. This phenomenon was likely due to the existence of GSSG and GSH from the Rev-CalB cell-free reaction (step 1). When capsid was produced with a buffer containing a mixture of GSSG and GSH, the amount of soluble CP production decreased.

For enzyme encapsulation, a fixed amount of RNA aptamer (10 μg) was added to the capsid CFPS reaction (step 2). After purification of the capsid, autoradiogram analysis showed that there is a significant difference between Rev-CalB encapsulation, with and without the RNA aptamer. The capsid CFPS with RNA aptamer sample had the Rev-CalB protein band while the capsid CFPS without the aptamer showed no Rev-CalB protein band (Figure 2-3A).

To see if guest molecules were randomly encapsulated during the capsid assembly, capsid was expressed in a cell extract where the sfGFP was overexpressed with a concentration of 2.0 mg/mL. Expressed capsids were purified via a size exclusion column. The chromatogram

showed that only the free sfGFP containing fractions showed a fluorescent signal, which indicates chances for guest molecules to be encapsulated without an affinity to the capsid are very low (Figure 2-4).

We tested enzyme encapsulation efficiency by adding various amounts of Rev-CalB but a fixed amount of RNA aptamer. Densitometry analysis showed that the higher the amount of Rev-CalB, the higher the number of enzyme encapsulation (Table 2-1). More than 1.7×10^1 µg of the enzyme significantly decreased total soluble VLP production (data not shown). Also, lower than 8.4×10^1 µg of enzyme did not show a detectable amount of protein band in densitometry analysis. An average of 6.5 Rev-CalB per capsid was the maximum encapsulation when 6 µM of the enzyme was present. Our results showed that only 28% of the total amount of Rev-CalB

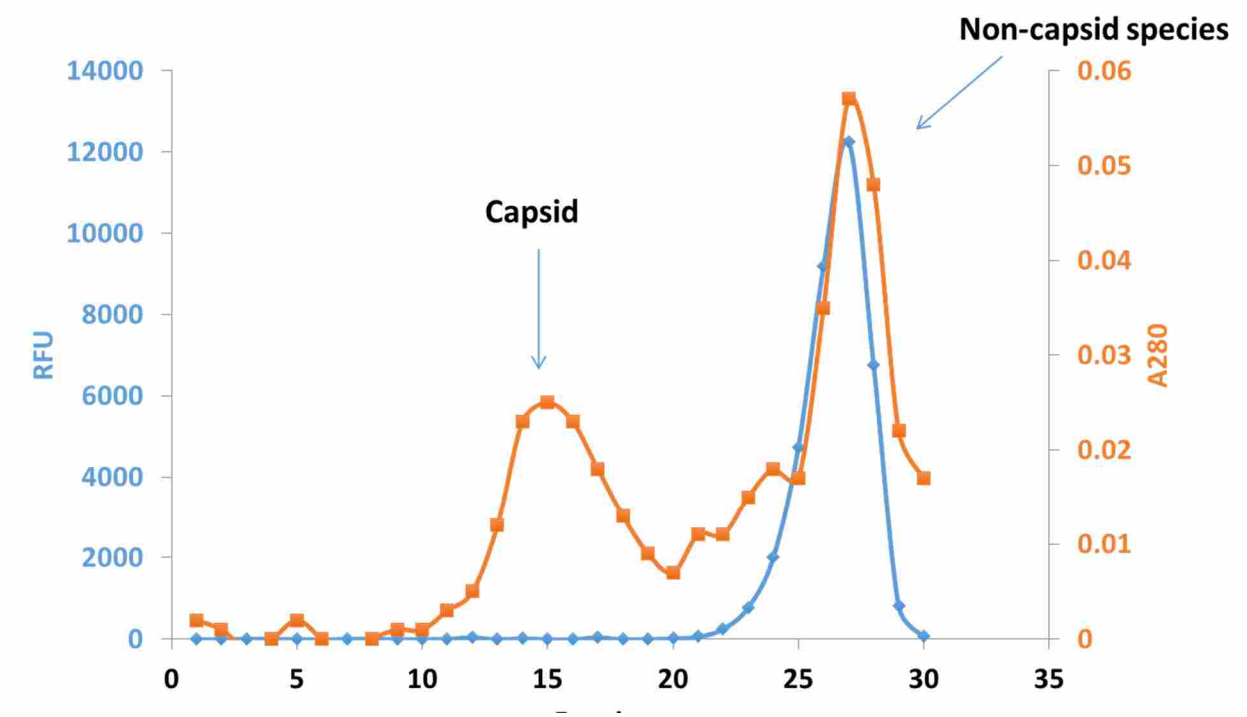

Figure 2-4 Size Exclusion Purification of Qβ VLP Assembled from CFPS Reaction with sfGFP
The VLP was expressed and assembled in the CFPS reaction where high concentration of sfGFP was present. The VLP expressed CFPS reaction was loaded on a size exclusion column (Sephacryl S400 HR) and purified by size. Each fraction collected 4 mL of the sample. The orange line represents absorbance at 280 nm and indicates protein content, while the blue line represents the fluorescence and indicates GFP content.

added were encapsulated, as the rest were found in the flow through sample. This is presumably due to steric hindrance. As the CalB is encapsulated, it inhibits the capsid assembly when an upper limit is reached. It is possible that the length of the aptamer may play a role in encapsulation efficiency as it is 646 nucleotides long. Shorter aptamers may help sequestering more guest enzymes. Another possible explanation is that the total capsid protein production level significantly drops upon transferring the CalB CFPS reaction. In addition, the CFPS reaction contains the glutathione buffer mix, and it reduces the soluble capsid production level (results not shown). Enzymes that do not require the glutathione buffer mix may increase the maximum encapsulation efficiency.

For TEM analysis, both samples were negatively stained with 0.2% phosphotungstic acid. Although the filled capsid showed a less stained inner surface, it was difficult to distinguish the filled from the empty capsids, which is in accord with previously reported data (Figure 2-3.B).[46] Both capsids had a mean diameter of 27 nm, similar to a previous report (Table 1).[66]

2.2.4 Enzyme Activity

To test the functional capabilities of the encapsulated lipases, activities of both free and encapsulated enzymes were compared using the chromogenic substrate 4-nitrophenyl octanoate (Figure 2-5).[84] The kinetic data from standard Michaelis-Menten analysis showed that both the free and encapsulated enzymes possess similar parameters with k_{cat}/K_M values of $3.1 \times 10^3 M^{-1}s^{-1}$ and $2.4 \times 10^3 M^{-1}s^{-1}$ for the free and the encapsulated lipases, respectively (Figure 2-5). They differ by less than a factor of two. The enzyme's turnover numbers were $7.1 \times 10^{-1}s^{-1}$and $3.3 \times 10^{-1}s^{-1}$ for the free and the encapsulated, respectively. The observed k_{cat} and k_{cat}/K_M values for both the free and the encapsulated enzymes were compatible to those

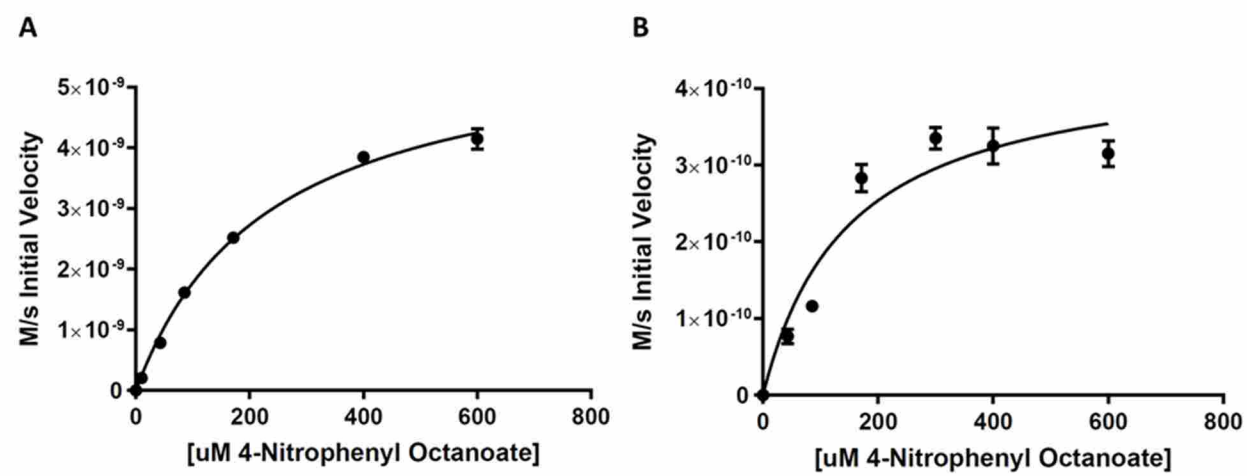

Free Rev-CalB
μmole/min/mg = $4.3 \times 10^{-1} \pm 0.06$
$K_M = 2.3 \times 10^{2} \pm 15\ s^{-1}$
$k_{cat} = 7.1 \times 10^{-1} \pm 0.02\ s^{-1}$
$k_{cat} / K_M = 3.1 \times 10^{3} \pm 120\ M^{-1}s^{-1}$

Encapsulated Rev-CalB
μmole/min/mg = $2.2 \times 10^{-1} \pm 0.02$
$K_M = 1.5 \times 10^{2} \pm 36\ s^{-1}$
$k_{cat} = 3.3 \times 10^{-1} \pm 0.03\ s^{-1}$
$k_{cat} / K_M = 2.4 \times 10^{3} \pm 350\ M^{-1}s^{-1}$

Figure 2-5 Kinetic Parameters of Free CalB and Encapsulated CalB Activity of both free and encapsulated CalB was measured with 4-Nitrophenyl octanoate as a substrate at 37˚C. **A** Free enzyme. **B** Encapsulated enzyme

reported for hydrolysis of 4-nitrophenyl ester substrates.[84] Specific activity of both the free and the encapsulated enzymes were 4.3×10^{-1} and 2.2×10^{-1} μmole/min/mg, respectively. Decreased K_M values were observed upon encapsulation. One possible explanation is that the structure of the Rev-CalB was slightly altered upon encapsulation, causing its substrate affinity to become stronger, thus making it harder for the enzyme to release the product. Decreased K_M and activity of an enzyme upon encapsulation was seen in a previous study as well.[45] Despite a decrease in activity, all encapsulated enzymes are assumed to be active, and the substrate and product are assumed to freely enter and exit the capsid through the fixed pores. Note that there was no detectable activity for the empty capsid (results not shown), which indicates the product conversion is solely contributed by the encapsulated lipase.

2.2.5 Enzyme Stability

VLP served as a shelter for the encapsulated Rev-CalB, and improved the resistance of CalB to high temperatures and a protease degradation. For the temperature inactivation test, both free and encapsulated enzymes were incubated at varying temperatures (37, 60, 75, and 90 ˚C) for 20 minutes before 1 hour incubation at the optimum temperature of 37 ˚C (Figure 2-6A).[85] Activities after each temperature stress were normalized by the activity at the optimum temperature. Almost all activity of the free enzyme was lost at 60 ˚C and above while the encapsulated enzyme maintained its full activity until 90 ˚C where it decreased only by 20%. The melting temperature of CalB is 57.7 ˚C.[86] We assumed that the free Rev-CalBs were denatured at 60 ˚C and above, and were subject to random aggregation. Returning to the enzyme's optimum temperature did not help its functionality, likely due to the loss of structure. On the other hand, encapsulated enzymes were immobilized at the inner surface of the capsid via the RNA aptamer. The capsid possesses a high melting temperature range of 85 – 100 ˚C.[87] It is assumed that the capsid protected the enzymes, and the enzymes seldom participated in aggregation due to the immobilization. When temperature returned to the optimum, enzymes retained its structure and gained its functionality.

VLP-protection of Rev-CalB was also tested by protease treatment. Both free and encapsulated enzymes were incubated at 37 ˚C with varying incubation times with proteinase K (Figure 2-6B). All activities were normalized by the activity before protease addition. Free enzyme activity dropped by a factor of 2 after 1 hour incubation of proteinase K, and only about 20% of the activity remained after 5 hour incubation with the protease. However, the encapsulated enzyme maintained its full activity over a 5 hour incubation with the protease. These data indicate that VLP provides protection and stability to guest molecules. Although there

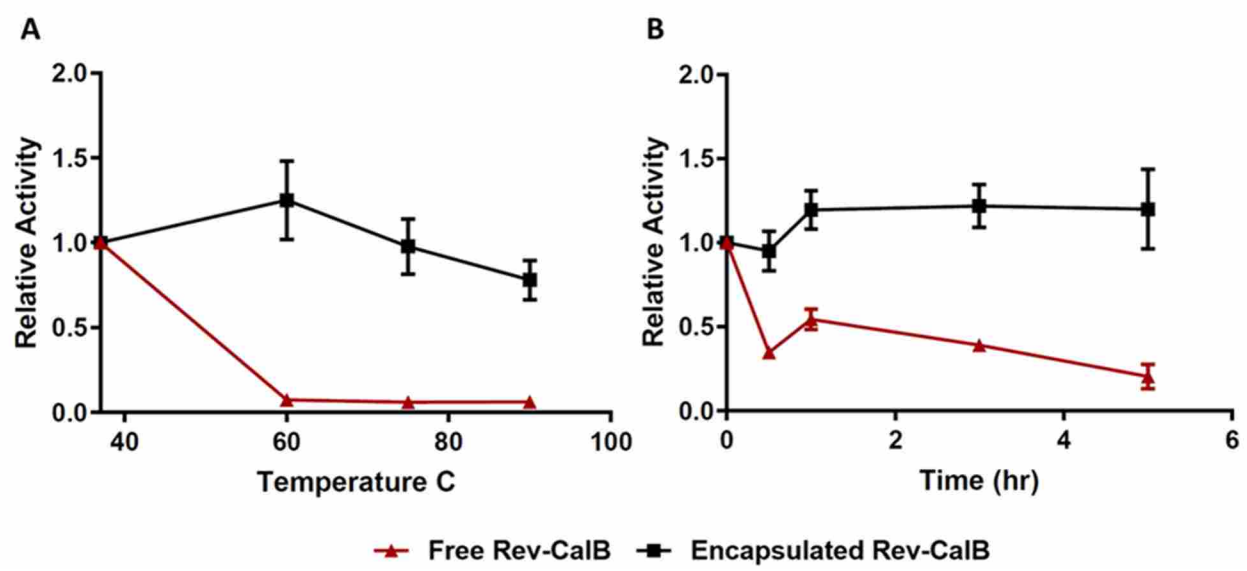

Figure 2-6 Protease and Temperature Inactivation Tests of the Free and Encapsulated Enzymes Both enzymes were exposed to high temperatures or proteinase K for the stability test. **A** High temperature inactivation. An immediate decrease in activity is observed for the free enzyme, while the encapsulated enzyme was stable even at 90˚C. **B** Protease inactivation. Unlike the free enzyme, the encapsulated enzyme showed activity even after the protease degradation.

was slight decrease in activity upon encapsulation, it was compensated by an increase in stability.

2.3 Conclusion and Future Directions

Here we have developed a simple *in vitro* two-step enzyme encapsulation method using CFPS. CFPS allows easy access to the Rev-CalB expression for optimization. The designed method does not require guest enzyme purification. The amount of guest enzymes for encapsulation determine encapsulation efficiency. The activity of the enzyme is largely intact upon encapsulation, and are stable against high temperatures and a protease.

A potential future direction for this research will be the increasing of the maximum encapsulation efficiency by optimizing the size of the RNA aptamer. The RNA aptamer used for the Rev-CalB encapsulation consists of the Qβ capsid sequence. This element can be removed

for it has no affinity to the Rev tag nor the capsid. On the other hand, different enzymes that do not require the glutathione buffer mix can be used.

Encapsulation of multiple enzymes for sequential reactions will be the next exciting future step. This study will enable us to understand enzymes in crowded cellular-like environments. Much like the carboxysome, a new biomimetic catalytic material can be constructed as well.

2.4 Materials and Methods

2.4.1 Extract Preparation

E. coli extract was prepared as previously reported using BL21 Star™ (DE3) *E. coli* strain purchased from Invitrogen (Carlsbad, CA).[88] Briefly, start culture of *E. coli* BL21 Star™ (DE3) strain grew in 5 mL of LB media for overnight with temperature of 37 ˚C at 280 rpm. The culture was transferred to 100 mL of LB media and grew until OD_{600} reached 2.0. The 105 mL culture was then transferred to 1 L media in Tunair flask. The addition of 1 mM of Isopropyl β-D-1-thiogalactopyranoside (IPTG) took place upon reaching 0.6 of OD_{600} to overexpress T7 RNA polymerase. Cells were harvested at the end of the exponential growth phase using centrifugation at 6000 RCF for 10 min at 4 ˚C. Cells were washed with icy Buffer A (10 mM Tris-acetate pH 8.2, 14 mM magnesium acetate, 60 mM potassium glutamate, and 1 mM dithiothreitol (DTT)) by centrifugation at 6000 RCF for 10 min at 4 ˚C. Cells were re-suspended with the buffer A (g of cell/mL of buffer A), and protein synthesis machinery was extracted using EmulsiFlex French Press homogenizer at 20000 psi. The homogenized cells were centrifuged at 12000 RCF for 30 min at 4 ˚C to clear the lysate. The supernatant was incubated

in a shaking incubator for 30 min at 280 rpm at 37 ˚C. The extract was flash-frozen in liquid nitrogen for one min before being stored at - 80 ˚C freezer.

Preparation of the cell extract for *Candida antarctica* lipase B (CalB) production was identical to the normal cell extract preparation described above, except BL21 Star™ (DE3) *E. coli* strain harboring pOFX-GroEL/ES plasmid a kind gift from Dr. Dong-Myung Kim (Chungnam National University, South Korea), and spectinomycin (100 μg/ml) was added to each culture media.

2.4.2 Cell-free Protein Synthesis

The CFPS reaction of bacteriophage Qβ coat protein (CP) was carried out in a 2.0 ml size eppindorf tube at 37 ˚C for 3 hours, with PANOxSP as an energy source. Each reaction contained 25% reaction volume of the cell extract, 1.2 nM plasmid, 12 to 15 mM magnesium glutamate, 1 mM 1,4-Diaminobutane, 1.5 mM Spermidine, 33.33 mM phosphoenolpyruvate (PEP), 10 mM ammonium glutamate, 175 mM potassium glutamate, 2.7 mM potassium oxalate, 0.33 mM nicotinamide adenine dinucleotide (NAD), 0.27 mM coenzyme A (CoA), 1.2 mM ATP, 0.86 mM CTP, 0.86 mM GTP, 0.86 mM UTP, 0.17 mM folinic acid, and 2 mM of all 20 amino acids except glutamic acid.

Rev-CalB expression was identical to CP expression, except the cell extract had overexpressed GroEL and GroES. A 5 mM glutathione buffer (GSSG : GSH = 4 : 1) was also added to the CFPS reaction at 30˚C for 5 hours.

2.4.3 Measuring Protein Concentration

Protein concentration was determined as previously described.[89] Briefly, 5 μM of radiolabeled (U-14C) Leucine (PerkinElmer, Waltham, MA) was added to the CFPS reaction. 3 μL of the CFPS reaction was spotted on each of the three separate pieces of Whatman 3MM chromatography paper and dried at 37˚C. Spotted papers were placed in a beaker on ice and covered with 5% (v/v) TCA at 4˚C to precipitate the proteins onto the filter paper for 15 min. The solution was exchanged with fresh TCA solution three times. Following the TCA washing steps, the papers were dried at 37˚C. Radioactivity of both TCA-precipitated and non-TCA-precipitated samples was measured using a LS6500 Multipurpose Scintillation Counter (Beckman Coulter, Brea, CA). The fraction of incorporated leucine in washed and unwashed protein were used to determine the amount of protein synthesized. Soluble yields were determined by sample centrifugation at 4˚C and 17,000 x g for 15 min, followed by TCA-precipitation and scintillation counting of the supernatants.

2.4.4 Bacteriophage Qβ Coat Protein Purification

Cell-free reaction that produced Qβ coat protein was inserted into a dialysis tubing bag (Spectra/Por, Rancho Dominguez, CA) with molecular weight cut off of 6-8 kDa. The sample was immediately dialyzed against 300 mL NET buffer (150 mM NaCl and 20 mM Tris-HCl, pH 7.8) for 18 h at 4˚C with three buffer exchanges. Dialyzed samples were loaded directly onto the HisPur™ Ni-NTA spin column (Thermo Scientific, Rockford, IL) that was pre-equilibrated with NET buffer containing 10 mM imidazole. The column was equilibrated with sample proteins for 30 min at 4˚C. The column was washed with a NET buffer containing 10 mM imidazole (1.2 mL). Capsids were eluted with a NET buffer containing 500 mM imidazole (300 uL). Eluted samples were concentrated during dialysis in 500 mL NET buffer containing 40% glycerol.

2.4.5 Lipase Activity

All experiments were run in triplicate, and all kinetic data were analyzed with respect to the enzyme concentration. The activity and kinetics of free Rev-CalB (8.2 nM) and encapsulated Rev-CalB (2.13 nM) were analyzed with the substrate 4-nitrophenyl octanoate (Sigma Aldrich, Milwaukee, Wisconsin) using Synergy^{TM} Mx (BioTek, Winooski, Vermont). Enzyme kinetics were determined by using varying concentrations of the substrate (10, 42.8, 85.7, 171.4, 300, 400, 600 μM) that were prepared in a substrate buffer (0.4 M DMSN. 0.2% triton x-100. 1x PBS) by serial dilutions. 1 μL of each varying substrate concentration were added to 70 μL of lipase reaction solution (0.4 M DMSN. 0.2% triton x-100. 1x PBS, pH 7.0) at 37˚C and read immediately. The absorbance was read at 410 nm wavelength for hydrolyzed substrate, 4-Nitrophenol. Measurements were repeated at 20 sec intervals for 20 min after 30 sec of shaking. The rate of substrate hydrolysis was determined at each substrate concentration using molar extinction coefficient of 17800 $M^{-1}cm^{-1}$ at 410 nm.

2.4.6 Thermal Stability

Enzymes were incubated at specific temperatures (37, 60, 75, and 90˚C) for 20 min using a thermocycler (Biorad, Hercules, CA), followed by incubation at 37˚C for an hour before the activity test. 1 μL of 12 mM substrate was added to each 70 μL lipase reaction solution. The substrate working concentration was 171.4 μM. Lipase concentrations of both free and encapsulated were 8.2 μM and 2.13 μM, respectively.

2.4.7 Protease Stability

To test enzyme stability against proteases, Proteinase K was purchased from Thermofischer Scientific (Fairlawn, NJ). 100 μL stock solution was prepared in NET buffer

containing 40% glycerol with 20 mg of Proteinase K powder (0.2 mg/μL). The stock protease solution was diluted to a concentration of 0.002 mg/μL by serial dilution using the lipase reaction solution. Both free and encapsulated Rev-CalB were pre-incubated at 37˚C for an hour before adding the protease. They were then incubated with Proteinase K for 0, 30, 60, 180, and 300 min at 37˚C. After the protease incubation, activity of the enzymes was measured with the substrate as described in 2.9.5.

2.4.8 Protein Separation and Autoradiography to Determine the Ratio of Capsid and Rev-CalB

Cell-free reaction product was subject to SDS-PAGE with 10% bis-tris gels (Invitrogen, Carlsbad, CA) for protein separation and stained with SimplyBlue SafeStain (Invitrogen). The PAGE gels were dried on a Whatman 3MM chromatography paper at 80˚C for 2 hours using a vacuum pump. The dried gels were exposed to Kodak BioMax MR autoradiography film (Rochester, NY) for 10 days. Densitometry measurements were performed using ImageJ software (National Institutes of Health). The capsid and Rev-CalB have different molecular weights (14 kDa - monomer and 37 kDa, respectively) and are found at different location in SDS-PAGE gel. Both capsid and enzyme are incorporated with C^{14}-leucine, and relative band intensities were used to measure the number of enzyme encapsulated per capsid.

2.4.9 Transmission Electron Microscopy (TEM)

Protein samples were dried on the formvar-coated copper grid (Electron Microscopy Sciences, Hatfield, PA) for 1 minute. The dried samples were soaked with 2% phosphotungstic acid for 1 minute and then dried. The images were digitally captured by Tecnai T-12 and Tecnai

T-20 TEM (FEI, Hillsboro, OR; Gatan, Pleasanton, CA) at 120 kV and 200 kV acceleration voltage, respectively. ImageJ software[90] sized images and scale bars.

2.4.10 Dynamic Light Scattering (DLS)

VLP's diameter was analyzed using DLS, 90Plus Particle Size Analyzer (Brookhaven Instruments, Holtsville, NY). Brookhaven Particle Size Analyzing software was used to calculate the mean diameters of VLPs.

3 CELL-FREE PROTEIN SYNTHESIS APPROACH TO BIOSENSING HUMAN ESTROGEN RECEPTOR BETA SPECIFIC ENDOCRINE DISRUPTORS

3.1 Introduction

Unintentional as well as intentional discharge of harmful chemicals into the environment has been the conventional reality of industrialized society for hundreds of years. In recent decades, an increasing wealth of evidence has shown a certain class of chemicals known as Endocrine Disrupting Chemicals (EDCs) to be harmful. Over 20 years ago, the EPA defined an EDC to be "an exogenous agent that interferes with the production, release, transport, metabolism, binding, action, or elimination of natural hormones in the body responsible for the maintenance of homeostasis and the regulation of developmental processes."[91] That same year, the EPA developed a screening program to identify potential EDCs. [92] Since that time, the EPA has screened 52 of the estimated 87,000 EDCs. [92] Studies detect significant levels of EDCs in air, land, drinking water, food, fuels, personal care products, pharmaceuticals, and synthetic hormones, and suggest that EDC exposure likely contributes to acute and chronic conditions including cancer, diabetes, obesity, metabolic syndrome, infertility, learning disabilities, and permanent brain damage.[93-94] A recent report estimated an EDC-exposure disease burden of $340 billion USD in the United States and $209 billion USD in the EU. [95]

One class of EDC's known as xenoestrogens (XEs) interferes specifically with the function of estrogen. Research has linked exposure to XEs with obesity and birth defects including DNA

methylation and placental alteration. [96-99] Bisphenol A (BPA) is a XE that has been used in plastic consumer products since 1957. Recent statements from the National Institute of Health[100] and the National Toxicology program[101] based on extensive literature review indicate that exposure to BPA may cause altered prostate, neurodevelopmental, and behavioral disorders.[98, 102] Research has linked BPA to the inhibition of downstream function in pituitary cells, decreased sperm viability, recurrent miscarriages, obesity, and ovarian dysfunction.[102] Additional studies linked BPA to emotional and behavioral problems in children. [103] Evidence shows that exposure to Estradiol (E2), another common XE, affects primary and secondary sex characteristics of aquatic wildlife.[104] Diarylpropionitrile (DPN) is another XE with a high selectivity for ER beta.

Recent advances in biosensor technology incorporating new developments in material science, genetic engineering, and synthetic biology enable unprecedented detection of EDCs [94]. Many *in vitro* models facilitate the study of the mechanisms of action of EDCs. [105] EDCs have been measured in urine, human serum, blood, fetal cord serum, and maternal placenta serum. [106] LC/MS and GC/MS are common techniques used to detect EDCs. Other efforts in biosensing EDCs utilize impedimetric response elements [107] and DNA aptamer optical-based biosensors.[108] These novel approaches show promise for future applications in characterization of EDCs, yet they are often time and labor intensive and in many instances, cost prohibitive. For example, LC/MS and GC/MS methods require trained technicians and significant equipment capital investment (~$190,000). Even when equipment is available, a simple urine test costs about 40 USD. [103, 106, 109-111]

Among the most common methods for detecting XEs are whole-cell bioassays that utilize yeast, *E. coli*, and human cell lines.[112-113] These methods are reliable and sensitive, but their

complicated laboratory procedures and long assay durations indicate that a technology more suitable for rapid and in-field XE detection would be highly advantageous.

Detecting interactions with the human estrogen receptor (hER) is of particular pharmaceutical interest. The World Health Organization lists estrogen receptor modulators as "essential medicines" to treat infertility.[114] Selective Estrogen Receptor Modulators (SERM's) currently treat a variety of conditions associated with postmenopausal women's health, including infertility and breast cancer, and have even inhibited the Ebola virus.[115-116] A rapid screening technology for estrogen receptor modulators would be an invaluable tool to characterize, classify, and discover estrogen receptor-linked medicines.

In a previous study, we demonstrated a Rapid Adaptable Portable In-vitro Detection biosensor platform (RAPID) for determining EDC activity.[117] This biosensor platform relies on exploiting the basic cellular mechanism of EDC activity in the following manner: an allosterically activated fusion protein containing the ligand-binding domain of a nuclear hormone receptor (NHR) indicates the presence of ligands when synthesized in a cell free environment. If EDC ligands are present, they will bind to the NHR and produce a colorimetric signal. Unlike many emerging biosensor technologies, the RAPID biosensor is not analyte-specific. Rather, the sensor produces a straightforward colorimetric response in real-time if any chemical that interacts with the NHR is present in the sample. Our previous work demonstrated the utility of this biosensor to detect and screen EDCs that interact with the Human Thyroid beta receptor (hTR-β). In this work, we employ the Human Estrogen Receptor beta (hER- β) to expand the detection capabilities of the RAPID biosensor to include XEs. We further demonstrate increased yield of the biosensor protein in human blood and urine samples by adding RNAse inhibitors to the open and robust CFPS-biosensor reaction.

3.2 Results and Discussion

3.2.1 RAPID Biosensor Design for the hERβ

Previously, we introduced the RAPID biosensor for detecting ligands that interact with the human thyroid receptor β (hTRβ). The modular nature of this biosensor makes it a very flexible platform for expanding the applications of the biosensor to many other nuclear hormone receptors. Here we used this feature to quickly engineer the biosensor for biosensing hERβ-specific endocrine disruptors.

The biosensor protein construct consists of four domains. These domains include 1) maltose binding domain; 2) mini-intein domain; 3) NHR ligand binding domain; and 4) the reporter enzyme. To adopt the biosensor for hERβ-Specific ligands, we replaced the hTRβ with hERβ binding domain resulting in the fusion protein illustrated in Figure 3-1.

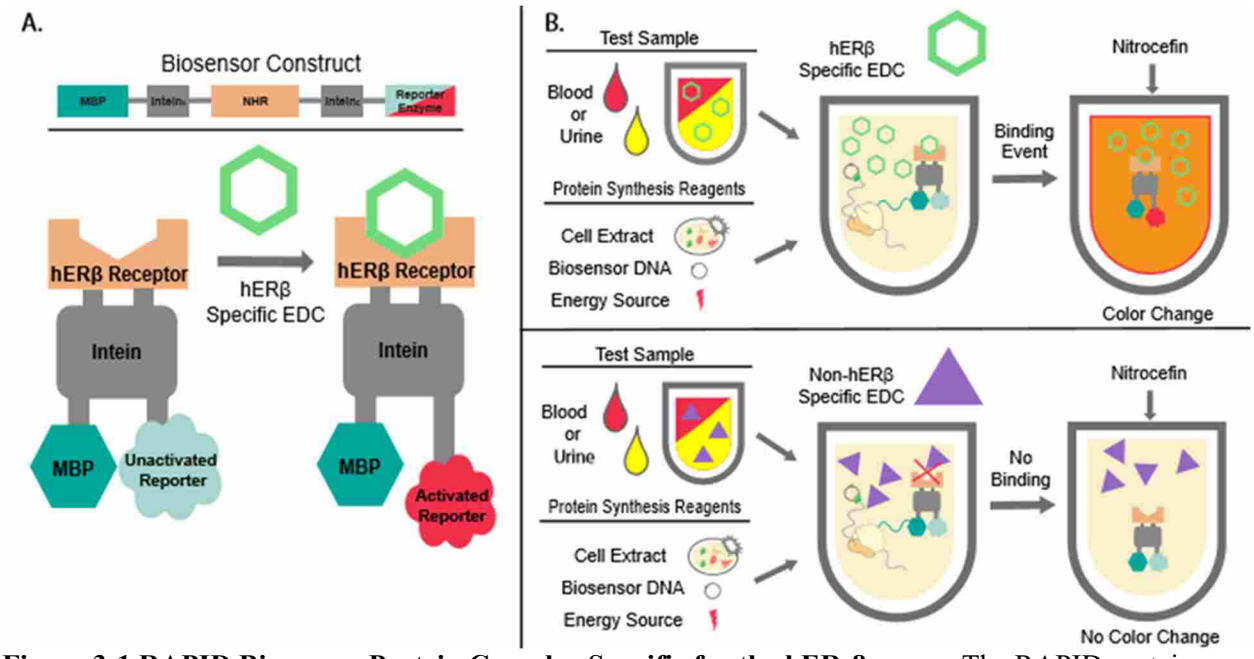

Figure 3-1 RAPID Biosensor Protein Complex Specific for the hER-β The RAPID protein complex changes its conformation slightly upon binding to hER-β specific ligands and enhances the reporter enzyme's ability to hydrolyze its substrate. The colorimetric assay can be measured only when hER-β specific ligands are present.

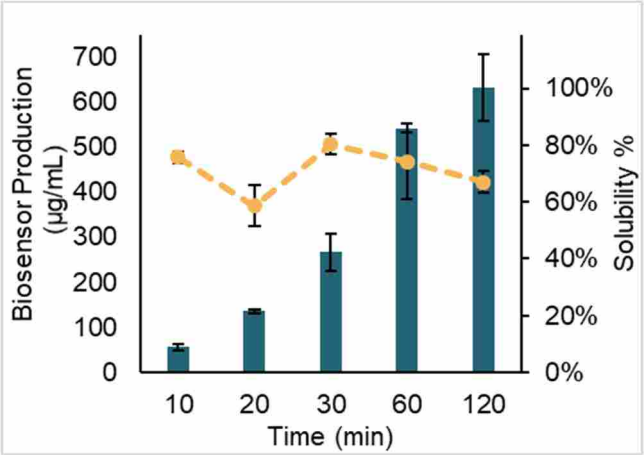

Figure 3-2 CFPS of the Biosensor Fusion Protein Protein production yield increases over the CFPS reaction time. The solubility level stays relatively constant with increasing protein concentration. (Bars represent total protein yield, error bars represent the standard deviation, and dashed line represents solubility percentage.)

It was hypothesized that the biosensor goes to the same conformational change as previously observed for hTRβ. This conformation change transfers to the reporter enzyme (β-lactamase) and makes it more accessible, which results in increased activity.

3.2.2 Cell-free Protein Synthesis of the Reporter Fusion Protein

The fusion protein, MBP-I_N-hERβ-I_C-β-lac, was expressed using CFPS system. The total protein production and solubility percentage were measured using incorporated C^{14} radiolabeled leucine as described in the materials and methods section. The results, as illustrated in Figure 3-2, showed successful expression of this 120 kD protein up to 650 µg/mL in 3 hr with an average solubility of 75%.

3.2.3 Hormone Biosensor Assay

The hormone biosensor assay includes a two-step processes: 1) expression of MBP-I_N-hTRβ-I_C-β-lac construct using CFPS in the presence of the ligands; and 2) performing nitrocefin colorimetric activity assay.

The biosensor was assessed in the presence of four endocrine disrupting compounds including E2, DPN, BPA, and TRIAC (Figure 3-3). E2, DPN, and BPA are known EDCs for estrogen nuclear hormone receptor with different binding affinity levels, all of which produced dose response graphs with excellent quality (Z' factor was between 0.5 to 1). The EC_{50} for E2, DPN, and BPA were 124, 71, and 1443 nM, respectively, which corresponds well with our previous

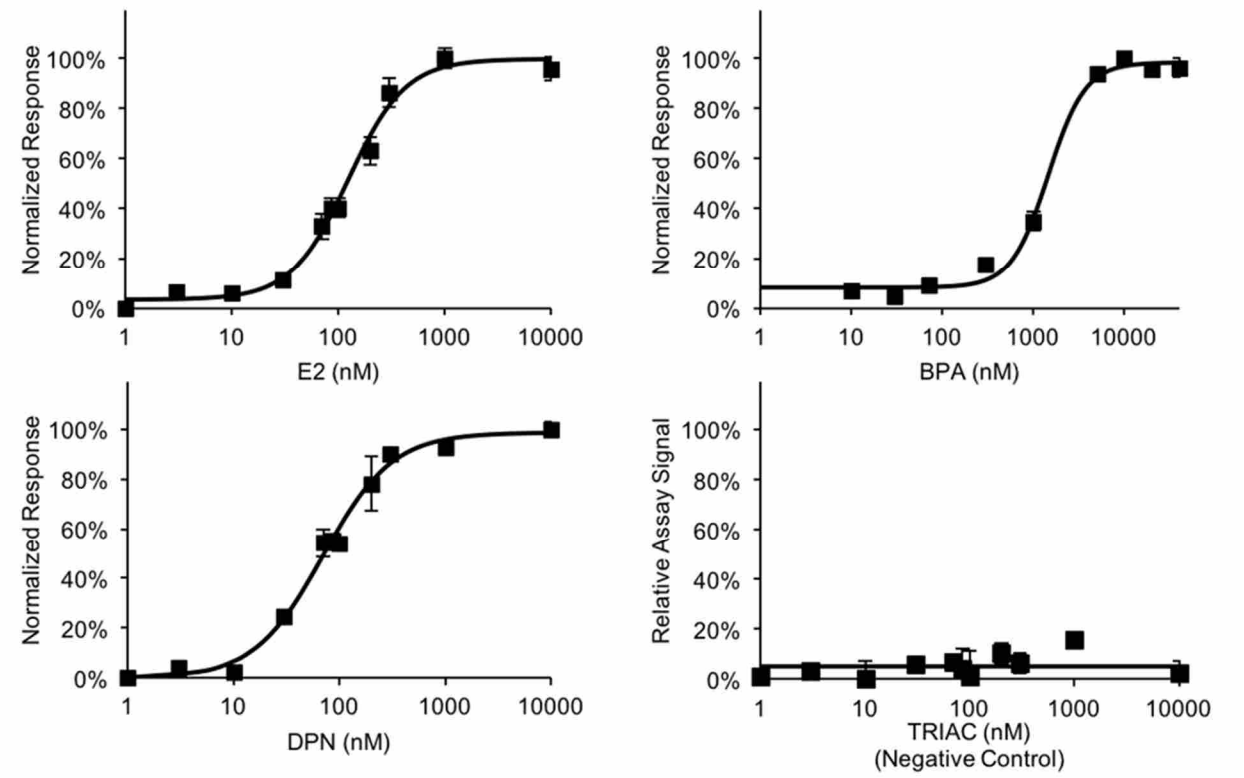

Ligands	EC50 (nM)	Z’	S/N	S/B	LOD (nM)
E2	124	0.83	179	3.1	26
DPN	71	0.82	36	2.9	9
BPA	1443	0.78	32	2.1	330
Triac	n/d	-24	0.3	1	n/d

Figure 3-3 Dose-response graphs and statistical analysis results for the RAPID biosensor in the presence of E2, DPN, BPA, and TRIAC The EC50 represents half-maximal effective concentration, Z' factor represents assay quality, S/N is signal to noise ratio, S/B is signal to background ratio, and LOD is limit of detection. The solid line represents fitted nitrocefin conversion values, the square markers represent the measured values, and the error bars represent one standard deviation for n=2.

study using a similar *in vivo* bacterial biosensor, 150, 170, and 1700 nM, respectively.[118] The negative control, TRIAC (a known EDC against hTRβ but not hERβ), didn't generate a statistically significant result, which indicates the specificity of the assay.

The total time to perform the biosensor assay was 2.5 hr (2 hr performing CFPS and 30 reading colorimetric assay), which is an order of magnitude less than our bacterial biosensor and other cell based nuclear hormone receptor biosensor with the same level of sensitivity. Also our CFPS-based-estrogen-specific biosensor could detect estrogen-receptor-specific EDCs. The limit of detection of each EDC varied from one another over the nM scale and relates to the EDC's binding efficiency and toxicity level. In case of BPA, FDA banned BPA-based baby plastic products including bottles, sippy cups, and infant formula packaging since 2012. BPA became a serious threat to human. While the EPA establishes the NOAEL (No Observed Adverse Effect Level) for BPA at 50 μg/kg of body weight/day, experts continue to debate the exact definition of a "safe" exposure threshold for BPA.[119] With the current analytical method, as low as 0.4 nM of BPA can be detected.[120] Efforts to improve the sensitivity level of the sensor will further enhance its utility.

3.2.4 Optimizing CFPS for Human Samples

In this work, we optimized the CFPS system to improve the performance of the system in the presence of human samples. Although a low amount of protein synthesis level is sufficient for biosensor assay, increasing the protein production yield in the presence of higher concentration of samples can result in improving the limit of detection EDCs and hormones in blood and urine samples.

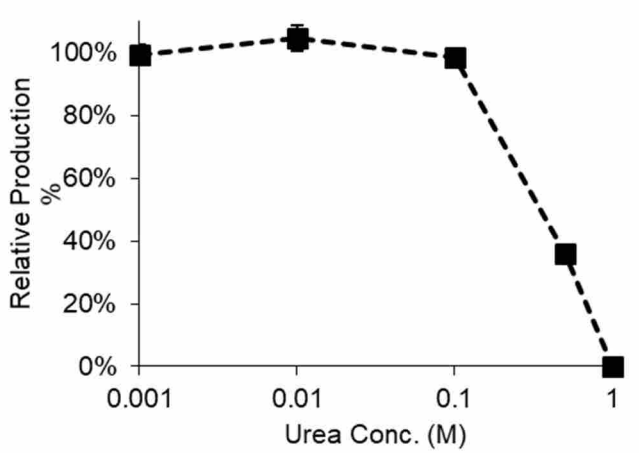

Figure 3-4 Effect of urea on CFPS of GFP CFPS activity level starts decreasing at urea concentration higher than 0.1 M. Error bars represent one standard deviation for n=3.

For the urine sample, it is hypothesized that urea is the main component that hinders protein synthesis. The urea concentration in human samples is in a range of 0.1 ~0.8 M[121-122] with an average of 0.22 M.[123] To see the effect of urea in CFPS, we performed CFPS with the model protein GFP in the presence of urea at concentrations between 0.001 to 1 M as shown in Figure 3-4. The results revealed that 0.1 M urea doesn't have significant effect on CFPS performance. Even at 0.5 M urea, still 40% protein synthesis capability was retained. Note that our previous result showed 10% urine, containing ~0.02 M urea, can eliminate CFPS.[124] So, the result suggested that urea in urine is not the main component that inactivates the CFPS activity.

We then hypothesized that there is a potential of RNAse activity in both urine and blood samples according to the literature, which can hinder protein synthesis.[125-127] To test this hypothesis, murine RNase inhibitor was added to the CFPS of GFP in addition to the urine and blood and containing as shown in Figure 3-5. Results revealed significant improvement in protein synthesis. For instance, for 20% by volume urine sample, the GFP production yield was jumped from less than 10% to more than 30%. The improvement was more significant for blood sample, as 10% by volume blood eliminated protein synthesis, but even 45% by volume blood in CFPS containing RNAse inhibitor retained 50% protein synthesis yield. The results correlate

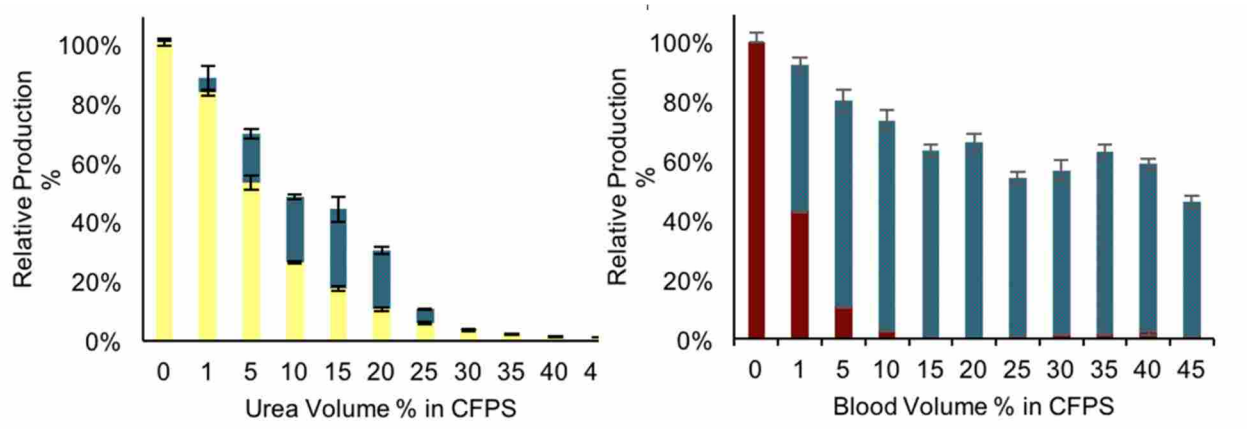

Figure 3-5 Effect of RNase inhibitor on CFPS of GFP in presence of urine (left chart) and blood (right chart) The dark bars in both graphs represent the improving effect of RNase inhibitor on protein production of CFPS in presence of both urine and blood. The error bars represent one standard deviation for n=3.

with the expected high RNAse activity in the blood sample and lesser activity in the urine sample. Using RNAse inhibitor in CFPS gives us the ability of adding up to 25% and 45% by volume urine and blood, respectively, and produces a sufficient amount of protein for biosensor assay. These higher volume percentage of samples help to detect lower concentration of ligands in samples. Note that RNAse concentration of human samples vary from person to person. Both urine and blood samples for this experiment were from different donors compared to our previous study. 1% urine could reduce the CFPS activity by 80% in our previous data[124] while the same amount of urine reduced CFPS activity by only 20% in this study. With blood sample, even 1% could reduce more than 50% CFPS activity in this study while the same amount did not have much effect on our previous CFPS activity.

3.2.5 NHR RAPID Biosensor Performance in Human Samples

We chose 10% and 20% by volume of urine and blood, respectively, to investigate the robustness of biosensor assay in the presence of these human samples. The results, Figure 3-6, showed that biosensor assay can generate dose response with EC_{50} of 15 and 35 nM for E2 in presence of urine and blood, respectively, and the assay quality was excellent for both samples

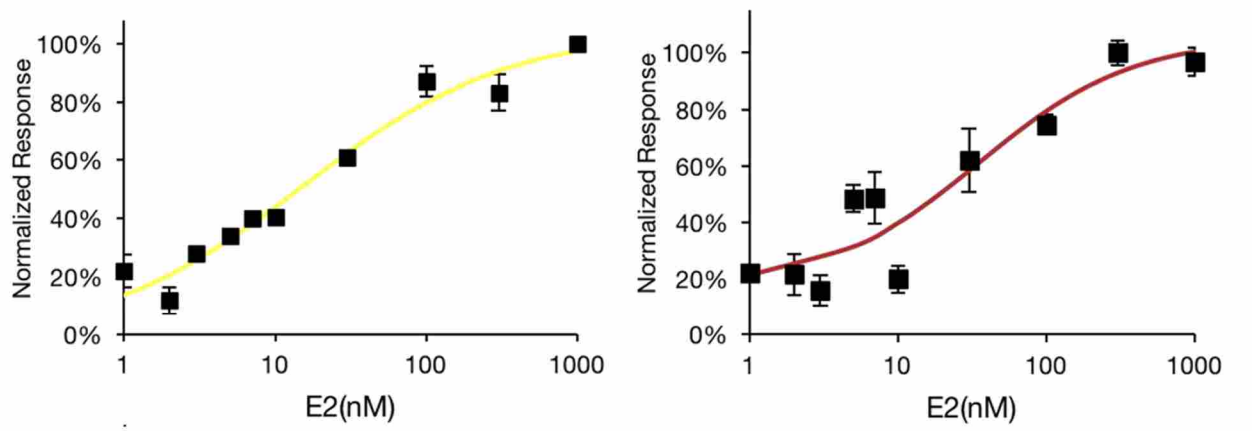

Sample	EC50 (nM)	Z'	S/N	S/B	LOD (nM)
Urine	15	0.78	21	1.5	4
Blood	35	0.78	12	1.5	8

Figure 3-6 Dose-response graph and statistical analysis results for the RAPID biosensor in the presence of E2 and 20% by volume blood and 10% by volume urine. The solid line represents fitted nitrocefin conversion values, the square markers represent the measured values, and the error bars represent one standard deviation for n=2.

(Z'=0.78). The EC_{50} is lower than the assay without urine and blood (Figure 3-3), which is similar to the result we observed for raw sewage in our previous study with thyroid nuclear hormone receptor biosensor.[124] It is hypothesized that lower CFPS yields can increase sensitivity by reducing the background. However, the signal to background is also reduced (compare Figure 3-5 and 3-6)

3.3 Conclusion and Future Directions

Here we demonstrated EDC detection in human blood and urine samples using our RAPID biosensor platform. The RAPID platform with human estrogen receptor β (hERβ) binds well with known hERβ EDCs. E2 detection in human blood and urine samples were aided by RNAse inhibitor.

Continued pursuit of this research is being carried out in Dr. Bradley Bundy's lab with emphasis on increasing the sensitivity of the RAPID biosensor.

3.4 Materials and Methods

All ligands were purchased from Sigma-Aldrich: diarylpropionitrile (DPN), bisphenol A (BPA), β-estradiol (E2), and triac. The blood was purchased from Innovative Research (Peary Ct, Novi, MI). The human donor urine was donated by the BYU health center. Nitrocefin was purchased from Cayman Chemical.

3.4.1 Biosensor Design and Construction

The pDB-MI (CI)-hERβ-β-lac construct borrowed the template of our previous biosensor construct. The pDB vector that encodes for the biosensor protein complex possess four domains: maltose binding domain (MBD), human β-estrogen receptor (hER-β), β-lactamase, and two inteins between MBD or CBD and hER-β, and hER-β and β-lactamase. This construct utilizes the T7 promoter to express proteins of interest. The construction of the vector is explained in our previous study

3.4.2 Hormone Biosensor Assay

The Hormone biosensor assay was performed in 2 stages. Stage 1: CFPS of the biosensor protein in 96 well plate for 20 min in the presence of 0 to 10 μM TRIAC, T3, or E2 dissolved in Dimethyl sulfoxide (DMSO). For consistency all CFPS reactions were adjusted to have 5 volume percent DMSO. Stage 2: After 20 min, the reactions were diluted 104-fold into PBS buffer, of which 25 μl was transferred into each well of a UV-transparent Corning® 96 well plate. The

104-fold CFPS dilution was introduced for optimal signal clarity and to eliminate overflow readings of our assay instruments, and was used in all experiments. To each well, 175 μl of 228.6 μM nitrocefin in PBS was additionally added to the wells at the same time to achieve a final nitrocefin concentration of 200 μM. The plates were then directly quantified via plate reader (BioTek Synergy Mx) for a nitrocefin-based beta-lactamase activity assay [128]. Specifically, the absorbance was read at 390 and 490 nm wavelengths for unreacted and reacted substrate nitrocefin, respectively. Measurements were repeated at 1 min intervals, with 10 sec shaking at each interval to mix, for 15 min. At the end of the assay, the absorbance was read at 760 nm to provide a relative background level for the assay. The rate of nitrocefin conversion was determined at each ligand concentration using the time course measurements, and the resulting rates were used to determine the half maximal effective ligand concentration (EC50).

3.4.3 Detection of Endocrine Disrupting Chemicals in Human Samples Using Biosensor Proteins

Each CFPS reaction containing EDC's and blood or urine was 8-fold diluted with PBS. This diluted CFPS reaction was further diluted with PBS and nitrocefin mixture (final 32- and 64-fold dilution for urine and blood, respectively). Both initial and Final nitrocefin concentration was 20 mM and 114.3 nM, respectively. The activity of the reporter protein (β -lactamase) was measured by plate reader (BioTek Synergy Mx) using both 390 and 490 nm wavelengths for substrate and product, respectively. Also 760 nm wavelength was used as a relative background. Samples were agitated for 10 seconds before the absorbance was measured each minute for 40 to 60 minutes. The rate of the reporter protein activity was used to determine half maximal effective ligand concentration (EC50).

3.4.4 Analysis of Hormone Biosensor Assay Results

Nitrocefin conversion value (NCV) was calculated based on the equation 3-1. A390, A490, and A760 were used for the yellow nitrocefin substrate, red converted product by β-lactamase, and background absorbance, respectively. To maximize the signal to noise ratio, each time point with the maximum difference between the negative control's NCV and the maximum ligand concentration was selected to get the dose response curve. To calculate the half maximal effective concentration, the Four-Parameter Logistic Function (equation 3-2) was used. [129] Parameters "a", "b", and "k" define lower/upper plateau values of the function and the slope factor, respectively.

Equation 3-1

$$Nitrocefin\ conversion\ value\ (NCV) = \frac{A490-A760\ (median\ of\ all\ reaction\ wells)}{A390-A760\ (median\ of\ all\ reaction\ wells)}$$

Equation 3-2

$$Predicted\ NCV = a + \frac{b-a}{1 + (\exp\big(k(\log(ligand\ concentration) - \log(EC50))\big))}$$

The normalized percent dose response was calculated using equation 3-3.

Equation 3-3

$$Normalized\ percent\ dose\ response = \frac{NCV - \min NCV}{\max NCV - \min NCV}\ X\ 100\%$$

The overall quality of the assays was determined by Z' factor, S/N, and S/B parameters. These parameters were calculated using previously studied method.[130-131] The limit of detection (LOD) was calculated by addition of 3SD (standard deviation) of the background signal to the mean of the background signal, which is based on IUPAC methodology.[132]

4 MULTI-DISULFIDE BOND PROTEIN EXPRESSION IN CELL-FREE PROTEIN SYNTHESIS

4.1 Introduction

Biosimilars are biological products approved for usage based on its highly similar functions with FDA-approved biological products (reference products). Recently, the Patient Protection and Affordable Care Act (Affordable Care Act) replaced the Public Health Service Act (PHS Act) for biosimilars to get faster licensing through a part of the Biologics Price Competition and Innovation Act law.[133] This movement encourages pharmaceutic companies to speed up biosimilar production. Although a significantly high amount of time and money is required, development and introduction of biosimilars into the market is beneficial in terms of cost savings, increased patient accessibility, and biosimilar innovation. Biosimilars are introduced in the market with prices 10-30% lower than that of reference products.[134] In the US, there is an estimated cost saving of up to $378 billion over the next 20 years with the introduction of biosimilar to the market.[135]

Tissue plasminogen activator (tPA) is a commercially available reference product. It is a serine protease that activates plasmin to dissolve various blood plasma proteins including fibrin blood clot. It has a total of 35 cysteine residues, allowing the formation of 17 disulfide bonds,[136-138] and consists of 527 amino acids with five domains (such as Kringle I, Finger, EGF, thrombolytic Kringle II, and protease domains).[139] It also treats stroke, the third leading cause of

death in US.[140] The mortality rate of ischemic stroke patients has a range of 13 and 15% within 30 days.[141] Currently, tPA is produced in CHO cells, but is not cost effective.[142] Other eukaryotic cell expression of the tPA struggle due to poor export, hyperglycosylation, and incorrect folding.[143-145] Attempts to produce tPA in periplasm of *E. coli* suffered from rare codon usage, mis-folding, and loss of function.[137-138] Also, an engineered *E. coli* (Origami B, DE3 strain) where two thioredoxins (TrxA and TrxC) and three glutaredoxins were oxidized, was used to express a full length of tPA.[136] However, there was no mention of the amount of tPA produced and specific activity of it.

Here we demonstrate the expression of tPA in our *E. coli* cell based cell-free protein synthesis (CFPS) using a buffer containing glutathione mix and prokaryotic disulfide bond C (DsbC) protein. DsbC is a disulfide bond isomerase and acts as a chaperon. It plays a role in proper protein folding by breaking the protein's non-native disulfide bonds.[146-148] tPA expression in the CFPS, specific activity, and blood clot lysis assay are discussed.

4.2 Results and Discussion

4.2.1 tPA Expression and Activity

To facilitate expression and proper folding of tPA, the glutathion buffer (described in Chapter 2) and the cell extract that contains overexpressed GroEL/ES and DsbC were added to the reaction. We first expressed tPA at 30˚C for 5 hours in comparison to 37˚C expression. Concentration of the DsbC added was 3.2 μM for both expressions. Only 32% and 36% of total protein produced at 37˚C and 30˚C, respectively, were soluble. Increased amounts of DsbC (6.5 μM) resulted in maximum total and soluble protein yields. Interestingly, CFPS reaction at 37˚C

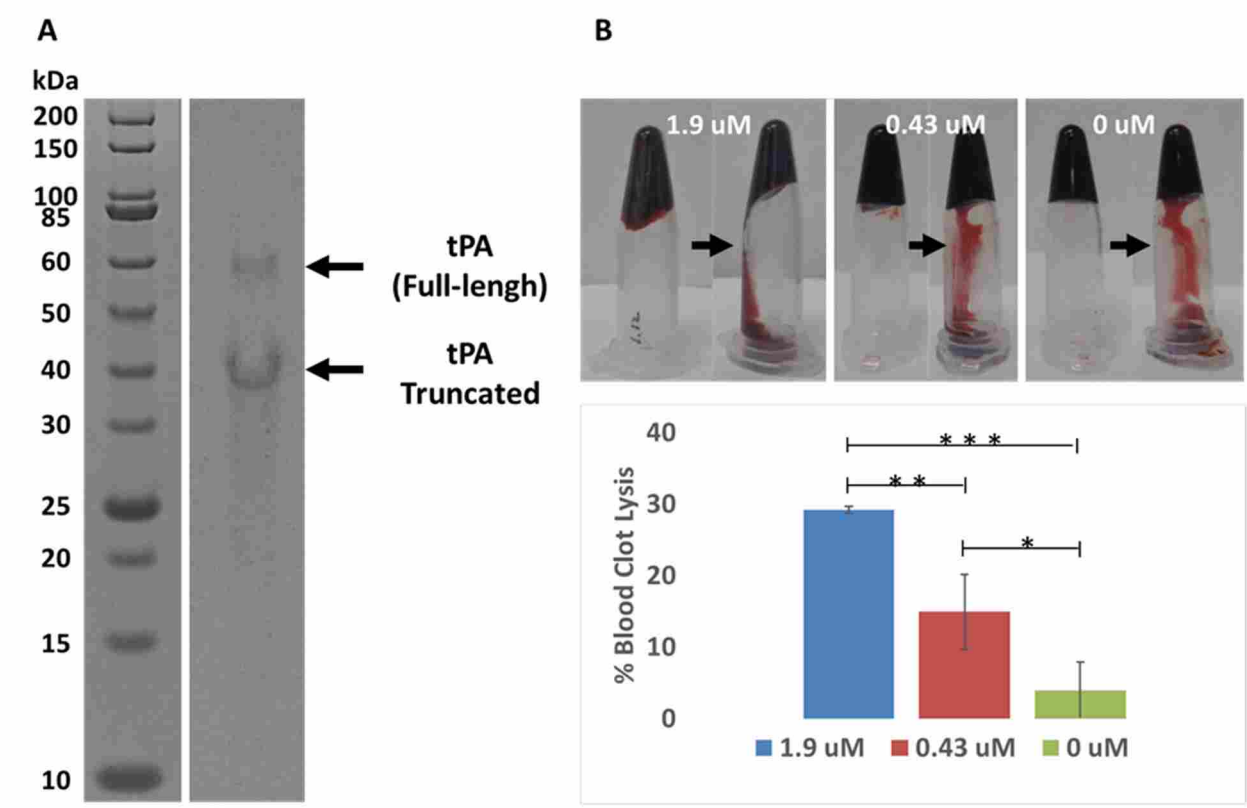

Figure 4-1 Purification and Activity of tPA Nickel affinity column purified tPA was separated by the SDS-PAGE and was exposed to the autoradiography film. It was also tested with a blood clot lysis assay. **A** Autoradiogram analysis showed both a full-length (63 kDa) and truncated tPA (about 40 kDa). **B** The CFPS expressed tPA lysed blood clot. *** = $P < 0.005$, ** = $P < 0.05$, and * = $P < 0.1$.

showed about 33% increase in both total and soluble tPA expressions. More than 84% of total proteins were soluble with the total soluble yield of 350 ng/µL in 70 µL reaction. The autoradiography analysis of pure tPA that was radiolabeled with C^{14}-Leu showed two protein bands that were exposed to the autoradiogram film (Figure 4-1).

Native tPA possesses a total of three glycosylation sites, namely, Asn 117, 184, and 448.[149] Studies have shown that native tPA gets cleaved by serine proteases to form a disulfide bond linked two-chain tPA when glycosylation is missing at Asn 184.[150-152] *E. coli* also has serine proteases[153] that cleave non-glycosylated tPA. Therefore, some of the expressed tPA was cleaved by the *E. coli* serine proteases, and the truncated tPA, cleaved at a location corresponding to Arg^{275}-Ile^{276} peptide bond,[151] was held by a nickel column. During the

purification process, slight basic condition buffer might reduce the disulfide bond, and the first 275 amino acid fragment could be eluted out.

The pure tPA was subject to its specific activity measurement using fluorogenic AMC substrate.[154] The specific activity of the tPA was 3.0×10^3 μmole/min/mg, which is slightly over 0.5% of the known activity of tPA.[138] Previous studies revealed that non full-length tPA possesses compatible activity[138, 155] compared to the full-length tPA, or 2-4-fold higher activity than that of the single chain tPA.[156] One possible explanation is that only 0.5% of all pure tPAs are folded correctly. tPA possesses 17 disulfide-bonds, so proper folding is challenging even with DsbC in *E. coli* cell extract.[136] Another reasoning is that they are correctly folded, but glycosylation is needed.

4.2.2 Blood Clot Lysis

Blood clot lysis activity of the pure tPA was tested (Figure 4). Three water samples were prepared with varying tPA concentrations (1.9, 0.43, and 0 μM). Each sample was added to coagulated blood for the lysis test. After overnight incubation at 37˚C, non-coagulated blood was cleared, and weights of the rest were measured. The highest amount of clot lysis resulted from the sample with 1.9 μM tPA. About 30% of the coagulated blood was lysed by that amount of protease. The clot lysis activity of the 1.9 μM and 0.43 μM samples were significantly different ($p < 0.05$). However, there was no significant difference between the 0.43 μM sample and the control. Based on the specific activity of the pure tPA, longer incubation may be required to carry out more significant clot lysis.

4.3 Conclusion and Future Directions

Our CFPS based tPA production level was 0.35 mg/mL, the highest of all reported studies with the full-length tPA production using *E. coli* cell extract. Endogenous serine proteases in the *E. coli* cell extract might have interacted with the expressed tPA and cleaved Arg (275)-Ile bond of the tPA.[150] The expressed tPA had a lower activity, possibly because glycosylation is missing, and/or only a small fraction of the expressed tPA was properly folded. Blood clot lysis assay showed that the expressed tPA could un-coagulate blood.

Studies showed that the locations of glycosylation determine the tPA activity.[156-157] Using the open nature of the CFPS, fusion of polyethylene glycol (PEG) on glycosylation sites by using unnatural amino acids can help increase the activity.

4.4 Materials and Methods

4.4.1 Extract Preparation

The preparation of cell extract of *E. coli* StarTM (DE3) strain harboring pOFX-GroEL/ES and pET-DsbC was identical to conventional extract preparation discussed in the chapter 2.9.1 with addition of spectinomycin (100μg/mL) and ampicillin (100 μg/mL).

4.4.2 Cell-free Protein Synthesis

The CFPS reaction of tPA was identical to the Qβ capsid except the cell extract had overexpressed GroEL/ES and DsbC. A 5 mM glutathione buffer (GSSG : GSH = 4 : 1) was also added to the CFPS reaction at 37˚C for 3 hours.

4.4.3 Measuring Protein Concentration

Chapter 2.9.3 explains the through process of measuring protein concentration

4.4.4 tPA Purification

The expressed tPA was dialyzed in the NET buffer (pH 6.7). The rest process was the same as described in 2.9.4.

4.4.5 tPA Activity

The SensoLyte AMC tPA activity assay kit was purchased from AnaSpec (Fremont, CA). The reaction buffer, AMC substrate, and standard AMC (fluorescence) were provided in the kit. Standard curve was plotted with varying concentration of the standard AMC. Pure tPA was added 1x reaction buffer that was provided to make total 50 μL of enzyme solution. 50 μL of the AMC substrate solution was added directly to the enzyme solution for the activity measurement. Fluorescence was monitored at excitation/emission = 354/442 nm.

4.4.6 Blood Clot Lysis Assay

Blood for the clot lysis assay was a donation from the BYU student health center. Aliquots of the blood were coagulated in the incubator at 37 ˚C for three hours. Non-coagulated blood was removed using an aspirator. Weight of the blood was measured before the incubation with tPA enzyme solution (1.9, 0.43, and 0 μM) in 100 μL of water. After 16 hours incubation with the tPA enzyme solution, the non-coagulated part was removed by using the aspirator, and the weight of the blood was measured. The % clot lysis was calculated using the equation 4-1.

Equation 4-1

$$\%\ clot\ lysis = \frac{Weight\ of\ Blood\ (Before\ Lysis) - Weight\ of\ Blood\ (After\ Lysis)}{Weight\ of\ Blood\ (Before\ Lysis)} \times 100\%$$

5 CONCLUSION

We demonstrated three applications of cell-free protein synthesis (CFPS): enzyme encapsulation, biosensing endocrine disrupting chemicals, and expression of a multi-disulfide bond protein. In each area of research, unique characteristic of CFPS was emphasized. CFPS provided a less time consuming and labor intensive platform for enzyme encapsulation. The conventional methods of both *in vivo* and *in vitro* enzyme encapsulation require fermentation and lysing cells. Purification steps for protein shells and guest enzymes are also important parts of enzyme encapsulation, which can take days or a week. CFPS-based simple *in vitro* enzyme encapsulation skipped the fermentation and guest enzyme purification steps, which saved time.

The open nature of CFPS enabled the expression of biosensor protein complex and selective detection of endocrine disrupting chemicals (EDCs) in the presence of blood and urine. EDCs did not fail the CFPS reaction of the biosensor protein complex, and the expressed protein folded correctly to specifically bind to the EDCs. EDC-bound protein complex had enzymatic activity against the substrate for the reporter enzyme. In addition, both blood and urine had RNAse activities, which is detrimental to our CFPS reaction. Addition of the RNAse inhibitor enabled CFPS to overcome nuclease activities that were found in blood and urine.

Expressions of functional bio-therapeutic proteins that have multi-disulfide bonds require a post translational modification system. Human protein expression in *E. coli* cells is difficult as they lack post translational modification function. CFPS can mimic the advanced cell-like

protein expression reaction with the help of a protein disulfide bond isomerase (DsbC), GroEL/ES, and a glutathione buffer mix. Both DsbC and GroEL/ES served as chaperonin-like proteins. The glutathione buffer mix changes the redox potential of the CFPS reaction. The buffer mix changed the CFPS reaction to a more oxidizing condition to facilitate disulfide bond formation.

REFERENCES

1. Carlson, E. D.; Gan, R.; Hodgman, C. E.; Jewett, M. C., Cell-free protein synthesis: applications come of age. *Biotechnology advances* **2012,** *30* (5), 1185-94.
2. Ma, Y.; Ghoshdastider, U.; Wang, J.; Ye, W.; Dotsch, V.; Filipek, S.; Bernhard, F.; Wang, X., Cell-free expression of human glucosamine 6-phosphate N-acetyltransferase (HsGNA1) for inhibitor screening. *Protein Expr Purif* **2012,** *86* (2), 120-6.
3. Salehi, A. S.; Smith, M. T.; Bennett, A. M.; Williams, J. B.; Pitt, W. G.; Bundy, B. C., Cell-free protein synthesis of a cytotoxic cancer therapeutic: Onconase production and a just-add-water cell-free system. *Biotechnol J* **2015**.
4. Park, C. G.; Kim, T. W.; Oh, I. S.; Song, J. K.; Kim, D. M., Expression of functional Candida antarctica lipase B in a cell-free protein synthesis system derived from Escherichia coli. *Biotechnology progress* **2009,** *25* (2), 589-93.
5. Jackson, A. M.; Boutell, J.; Cooley, N.; He, M., Cell-free protein synthesis for proteomics. *Brief Funct Genomic Proteomic* **2004,** *2* (4), 308-19.
6. Worsdorfer, B.; Woycechowsky, K. J.; Hilvert, D., Directed evolution of a protein container. *Science* **2011,** *331* (6017), 589-92.
7. Smith, M. T.; Wu, J. C.; Varner, C. T.; Bundy, B. C., Enhanced protein stability through minimally invasive, direct, covalent, and site-specific immobilization. *Biotechnology progress* **2013,** *29* (1), 247-54.
8. Wu, J. C.; Hutchings, C. H.; Lindsay, M. J.; Werner, C. J.; Bundy, B. C., Enhanced enzyme stability through site-directed covalent immobilization. *Journal of biotechnology* **2015,** *193*, 83-90.
9. Hong, S. H.; Kwon, Y. C.; Jewett, M. C., Non-standard amino acid incorporation into proteins using Escherichia coli cell-free protein synthesis. *Front Chem* **2014,** *2*, 34.
10. Sachse, R.; Dondapati, S. K.; Fenz, S. F.; Schmidt, T.; Kubick, S., Membrane protein synthesis in cell-free systems: from bio-mimetic systems to bio-membranes. *FEBS letters* **2014,** *588* (17), 2774-81.
11. Oza, J. P.; Aerni, H. R.; Pirman, N. L.; Barber, K. W.; ter Haar, C. M.; Rogulina, S.; Amrofell, M. B.; Isaacs, F. J.; Rinehart, J.; Jewett, M. C., Robust production of recombinant phosphoproteins using cell-free protein synthesis. *Nature communications* **2015,** *6*, 8168.
12. Junge, F.; Haberstock, S.; Roos, C.; Stefer, S.; Proverbio, D.; Dotsch, V.; Bernhard, F., Advances in cell-free protein synthesis for the functional and structural analysis of membrane proteins. *New biotechnology* **2011,** *28* (3), 262-71.
13. Wuu, J. J.; Swartz, J. R., High yield cell-free production of integral membrane proteins without refolding or detergents. *Biochimica et biophysica acta* **2008,** *1778* (5), 1237-50.
14. Zawada, J. F.; Yin, G.; Steiner, A. R.; Yang, J.; Naresh, A.; Roy, S. M.; Gold, D. S.; Heinsohn, H. G.; Murray, C. J., Microscale to manufacturing scale-up of cell-free cytokine

production--a new approach for shortening protein production development timelines. *Biotechnology and bioengineering* **2011,** *108* (7), 1570-8.
15. Kuchenreuther, J. M.; Shiigi, S. A.; Swartz, J. R., Cell-free synthesis of the H-cluster: a model for the in vitro assembly of metalloprotein metal centers. *Methods in molecular biology* **2014,** *1122*, 49-72.
16. Li, J.; Lawton, T. J.; Kostecki, J. S.; Nisthal, A.; Fang, J.; Mayo, S. L.; Rosenzweig, A. C.; Jewett, M. C., Cell-free protein synthesis enables high yielding synthesis of an active multicopper oxidase. *Biotechnol J* **2016,** *11* (2), 212-8.
17. Bundy, B. C.; Franciszkowicz, M. J.; Swartz, J. R., Escherichia coli-based cell-free synthesis of virus-like particles. *Biotechnology and bioengineering* **2008,** *100* (1), 28-37.
18. Smith, M. T.; Varner, C. T.; Bush, D. B.; Bundy, B. C., The incorporation of the A2 protein to produce novel Qbeta virus-like particles using cell-free protein synthesis. *Biotechnology progress* **2012,** *28* (2), 549-55.
19. Jewett, M. C.; Swartz, J. R., Mimicking the Escherichia coli cytoplasmic environment activates long-lived and efficient cell-free protein synthesis. *Biotechnology and bioengineering* **2004,** *86* (1), 19-26.
20. Ardelt, W.; Shogen, K.; Darzynkiewicz, Z., Onconase and amphinase, the antitumor ribonucleases from Rana pipiens oocytes. *Current pharmaceutical biotechnology* **2008,** *9* (3), 215-25.
21. Fiorini, C.; Cordani, M.; Gotte, G.; Picone, D.; Donadelli, M., Onconase induces autophagy sensitizing pancreatic cancer cells to gemcitabine and activates Akt/mTOR pathway in a ROS-dependent manner. *Biochimica et biophysica acta* **2015,** *1853* (3), 549-60.
22. Smolewski, P.; Witkowska, M.; Zwolinska, M.; Cebula-Obrzut, B.; Majchrzak, A.; Jeske, A.; Darzynkiewicz, Z.; Ardelt, W.; Ardelt, B.; Robak, T., Cytotoxic activity of the amphibian ribonucleases onconase and r-amphinase on tumor cells from B cell lymphoproliferative disorders. *International journal of oncology* **2014,** *45* (1), 419-25.
23. Ardelt, W.; Mikulski, S. M.; Shogen, K., Amino acid sequence of an anti-tumor protein from Rana pipiens oocytes and early embryos. Homology to pancreatic ribonucleases. *The Journal of biological chemistry* **1991,** *266* (1), 245-51.
24. Singh, U. P.; Ardelt, W.; Saxena, S. K.; Holloway, D. E.; Vidunas, E.; Lee, H. S.; Saxena, A.; Shogen, K.; Acharya, K. R., Enzymatic and structural characterisation of amphinase, a novel cytotoxic ribonuclease from Rana pipiens oocytes. *Journal of molecular biology* **2007,** *371* (1), 93-111.
25. Wang, Z.-G., Wan, L.-S., Liu, Z.-M., Huang, X.-J., Xu, Z.-K., Enzyme immobilization on electrospun polymer nanofibers: An overview. *J. Mol. Catal. B: Enzymatic* **2009,** *56*, 189-195.
26. Smith, M. T.; Wilding, K. M.; Hunt, J. M.; Bennett, A. M.; Bundy, B. C., The emerging age of cell-free synthetic biology. *FEBS letters* **2014,** *588* (17), 2755-61.
27. Shrestha, P.; Smith, M. T.; Bundy, B. C., Cell-free unnatural amino acid incorporation with alternative energy systems and linear expression templates. *New biotechnology* **2014,** *31* (1), 28-34.
28. Salehi, A. S.; Earl, C. C.; Muhlestein, C.; Bundy, B. C., Escherichia coli-based cell-free extract development for protein-based cancer therapeutic production. *Int J Dev Biol* **2016,** *60* (7-8-9), 237-243.
29. Sun, Y.; Cheng, J., Hydrolysis of lignocellulosic materials for ethanol production: a review. *Bioresource technology* **2002,** *83* (1), 1-11.

30. Kirk, O.; Borchert, T. V.; Fuglsang, C. C., Industrial enzyme applications. *Current opinion in biotechnology* **2002,** *13* (4), 345-51.
31. Dulieu, C.; Moll, M.; Boudrant, J.; Poncelet, D., Improved performances and control of beer fermentation using encapsulated alpha-acetolactate decarboxylase and modeling. *Biotechnology progress* **2000,** *16* (6), 958-65.
32. P. Molimard, H. E. S., Compounds Involved in the Flavor of Surface Mold-Ripened Cheeses: Orgins and Properties. *Journal of dairy science* **1996,** *79* (2), 169-184.
33. Guzman-Maldonado, H.; Paredes-Lopez, O., Amylolytic enzymes and products derived from starch: a review. *Critical reviews in food science and nutrition* **1995,** *35* (5), 373-403.
34. Rychlik, W.; Spencer, W. J.; Rhoads, R. E., Optimization of the annealing temperature for DNA amplification in vitro. *Nucleic acids research* **1990,** *18* (21), 6409-12.
35. Bajpai, P., Application of enzymes in the pulp and paper industry. *Biotechnology progress* **1999,** *15* (2), 147-57.
36. Begley, C. G.; Paragina, S.; Sporn, A., An analysis of contact lens enzyme cleaners. *Journal of the American Optometric Association* **1990,** *61* (3), 190-4.
37. Brockman, H. L.; Law, J. H.; Kezdy, F. J., Catalysis by adsorbed enzymes. The hydrolysis of tripropionin by pancreatic lipase adsorbed to siliconized glass beads. *The Journal of biological chemistry* **1973,** *248* (14), 4965-70.
38. Lu, X.; Zheng, X.; Li, X.; Zhao, J., Adsorption and mechanism of cellulase enzymes onto lignin isolated from corn stover pretreated with liquid hot water. *Biotechnol Biofuels* **2016,** *9*, 118.
39. Gonzalez-Saiz, J. M., Pizarro, C, Polyacrylamide gels as support for enzyme immobilization by entrapment. Effect of polyelectrolyte carrier, pH and temperature on enzyme action and kinetics parameters. *European Polymer Journal* **2001,** *37* (3), 435-444.
40. Sharma, M.; Sharma, V.; Majumdar, D. K., Entrapment of alpha-Amylase in Agar Beads for Biocatalysis of Macromolecular Substrate. *Int Sch Res Notices* **2014,** *2014*, 936129.
41. Mogharabi, M.; Nassiri-Koopaei, N.; Bozorgi-Koushalshahi, M.; Nafissi-Varcheh, N.; Bagherzadeh, G.; Faramarzi, M. A., Immobilization of laccase in alginate-gelatin mixed gel and decolorization of synthetic dyes. *Bioinorg Chem Appl* **2012,** *2012*, 823830.
42. Bhushan, B.; Pal, A.; Jain, V., Improved Enzyme Catalytic Characteristics upon Glutaraldehyde Cross-Linking of Alginate Entrapped Xylanase Isolated from Aspergillus flavus MTCC 9390. *Enzyme Res* **2015,** *2015*, 210784.
43. Yildirim, D.; Tukel, S. S.; Alagoz, D., Crosslinked enzyme aggregates of hydroxynitrile lyase partially purified from Prunus dulcis seeds and its application for the synthesis of enantiopure cyanohydrins. *Biotechnology progress* **2014,** *30* (4), 818-27.
44. Minten, I. J.; Claessen, V. I.; Blank, K.; Rowan, A. E.; Nolte, R. J. M.; Cornelissen, J. J. L. M., Catalytic capsids: the art of confinement. *Chem Sci* **2011,** *2* (2), 358-362.
45. Patterson, D. P.; Prevelige, P. E.; Douglas, T., Nanoreactors by programmed enzyme encapsulation inside the capsid of the bacteriophage P22. *ACS nano* **2012,** *6* (6), 5000-9.
46. Fiedler, J. D.; Brown, S. D.; Lau, J. L.; Finn, M. G., RNA-directed packaging of enzymes within virus-like particles. *Angewandte Chemie* **2010,** *49* (50), 9648-51.
47. Patterson, D. P.; Schwarz, B.; Waters, R. S.; Gedeon, T.; Douglas, T., Encapsulation of an enzyme cascade within the bacteriophage P22 virus-like particle. *ACS chemical biology* **2014,** *9* (2), 359-65.

48. Chen, H., Liu, L.-H., Wang, L.-S., Ching, C.-B., Yu, H.-W., Yang, Y.-Y., Thermally responsive reversed micelles for immobilization of enzymes. *Advanced Functional Materials* **2007,** *18* (1), 95-102.
49. Dwevedi, A., *Enzyme Immobilization: Advances in Industry, Agriculture, Medicine, and the Environment*. Springer International Publishing: 2016.
50. Cannon, G. C.; Bradburne, C. E.; Aldrich, H. C.; Baker, S. H.; Heinhorst, S.; Shively, J. M., Microcompartments in prokaryotes: carboxysomes and related polyhedra. *Applied and environmental microbiology* **2001,** *67* (12), 5351-61.
51. Cheng, S.; Liu, Y.; Crowley, C. S.; Yeates, T. O.; Bobik, T. A., Bacterial microcompartments: their properties and paradoxes. *BioEssays : news and reviews in molecular, cellular and developmental biology* **2008,** *30* (11-12), 1084-95.
52. Kerfeld, C. A.; Erbilgin, O., Bacterial microcompartments and the modular construction of microbial metabolism. *Trends Microbiol* **2015,** *23* (1), 22-34.
53. Yeates, T. O.; Kerfeld, C. A.; Heinhorst, S.; Cannon, G. C.; Shively, J. M., Protein-based organelles in bacteria: carboxysomes and related microcompartments. *Nat Rev Microbiol* **2008,** *6* (9), 681-91.
54. Kinney, J. N.; Axen, S. D.; Kerfeld, C. A., Comparative analysis of carboxysome shell proteins. *Photosynth Res* **2011,** *109* (1-3), 21-32.
55. Yeates, T. O.; Thompson, M. C.; Bobik, T. A., The protein shells of bacterial microcompartment organelles. *Current opinion in structural biology* **2011,** *21* (2), 223-31.
56. Axen, S. D.; Erbilgin, O.; Kerfeld, C. A., A taxonomy of bacterial microcompartment loci constructed by a novel scoring method. *PLoS Comput Biol* **2014,** *10* (10), e1003898.
57. Bonacci, W.; Teng, P. K.; Afonso, B.; Niederholtmeyer, H.; Grob, P.; Silver, P. A.; Savage, D. F., Modularity of a carbon-fixing protein organelle. *Proceedings of the National Academy of Sciences of the United States of America* **2012,** *109* (2), 478-83.
58. Cot, S. S.; So, A. K.; Espie, G. S., A multiprotein bicarbonate dehydration complex essential to carboxysome function in cyanobacteria. *Journal of bacteriology* **2008,** *190* (3), 936-45.
59. Fan, C.; Cheng, S.; Liu, Y.; Escobar, C. M.; Crowley, C. S.; Jefferson, R. E.; Yeates, T. O.; Bobik, T. A., Short N-terminal sequences package proteins into bacterial microcompartments. *Proceedings of the National Academy of Sciences of the United States of America* **2010,** *107* (16), 7509-14.
60. Adolph, K. W.; Butler, P. J., Assembly of a spherical plant virus. *Philos Trans R Soc Lond B Biol Sci* **1976,** *276* (943), 113-22.
61. Comellas-Aragones, M.; Engelkamp, H.; Claessen, V. I.; Sommerdijk, N. A.; Rowan, A. E.; Christianen, P. C.; Maan, J. C.; Verduin, B. J.; Cornelissen, J. J.; Nolte, R. J., A virus-based single-enzyme nanoreactor. *Nature nanotechnology* **2007,** *2* (10), 635-9.
62. Minten, I. J.; Hendriks, L. J.; Nolte, R. J.; Cornelissen, J. J., Controlled encapsulation of multiple proteins in virus capsids. *Journal of the American Chemical Society* **2009,** *131* (49), 17771-3.
63. Minten, I. J.; Nolte, R. J.; Cornelissen, J. J., Complex assembly behavior during the encapsulation of green fluorescent protein analogs in virus derived protein capsules. *Macromolecular bioscience* **2010,** *10* (5), 539-45.
64. Weber, H., The binding site for coat protein on bacteriophage Qbeta RNA. *Biochimica et biophysica acta* **1976,** *418* (2), 175-83.

65. Witherell, G. W.; Uhlenbeck, O. C., Specific RNA binding by Q beta coat protein. *Biochemistry* **1989,** *28* (1), 71-6.
66. Golmohammadi, R.; Fridborg, K.; Bundule, M.; Valegard, K.; Liljas, L., The crystal structure of bacteriophage Q beta at 3.5 A resolution. *Structure* **1996,** *4* (5), 543-54.
67. Fiedler, J. D.; Higginson, C.; Hovlid, M. L.; Kislukhin, A. A.; Castillejos, A.; Manzenrieder, F.; Campbell, M. G.; Voss, N. R.; Potter, C. S.; Carragher, B.; Finn, M. G., Engineered mutations change the structure and stability of a virus-like particle. *Biomacromolecules* **2012,** *13* (8), 2339-48.
68. Parent, K. N.; Khayat, R.; Tu, L. H.; Suhanovsky, M. M.; Cortines, J. R.; Teschke, C. M.; Johnson, J. E.; Baker, T. S., P22 coat protein structures reveal a novel mechanism for capsid maturation: stability without auxiliary proteins or chemical crosslinks. *Structure* **2010,** *18* (3), 390-401.
69. Teschke, C. M.; McGough, A.; Thuman-Commike, P. A., Penton release from P22 heat-expanded capsids suggests importance of stabilizing penton-hexon interactions during capsid maturation. *Biophys J* **2003,** *84* (4), 2585-92.
70. Anderson, E. M., Larsson, K. M., Kirk, O., One biocatalyst-many applications: the use of Candida antarctica B-lipase in organic synthesis. *Biocatal. Biotransform* **1998,** *16*, 181-204.
71. Blank, K.; Morfill, J.; Gumpp, H.; Gaub, H. E., Functional expression of Candida antarctica lipase B in Eschericha coli. *Journal of biotechnology* **2006,** *125* (4), 474-83.
72. Bornscheuer, U. T., Kazlauskas, R. J, Hydrolases in organic synthesis: regio- and stereoselective biotransformations. *Wiley-VCH* **1999**.
73. Uppenberg, J.; Hansen, M. T.; Patkar, S.; Jones, T. A., The sequence, crystal structure determination and refinement of two crystal forms of lipase B from Candida antarctica. *Structure* **1994,** *2* (4), 293-308.
74. Strzelczyk, P.; Bujacz, G. D.; Kielbasinski, P.; Blaszczyk, J., Crystal and molecular structure of hexagonal form of lipase B from Candida antarctica. *Acta Biochim Pol* **2016,** *63* (1), 103-109.
75. Kim, S. K.; Park, Y. C.; Lee, H. H.; Jeon, S. T.; Min, W. K.; Seo, J. H., Simple amino acid tags improve both expression and secretion of Candida antarctica lipase B in recombinant Escherichia coli. *Biotechnology and bioengineering* **2015,** *112* (2), 346-55.
76. Rotticci-Mulder, J. C.; Gustavsson, M.; Holmquist, M.; Hult, K.; Martinelle, M., Expression in Pichia pastoris of Candida antarctica lipase B and lipase B fused to a cellulose-binding domain. *Protein Expr Purif* **2001,** *21* (3), 386-92.
77. Larsen, M. W.; Bornscheuer, U. T.; Hult, K., Expression of Candida antarctica lipase B in Pichia pastoris and various Escherichia coli systems. *Protein Expr Purif* **2008,** *62* (1), 90-7.
78. Magnusson, A. O.; Rotticci-Mulder, J. C.; Santagostino, A.; Hult, K., Creating space for large secondary alcohols by rational redesign of Candida antarctica lipase B. *Chembiochem : a European journal of chemical biology* **2005,** *6* (6), 1051-6.
79. Qian, Z.; Lutz, S., Improving the catalytic activity of Candida antarctica lipase B by circular permutation. *Journal of the American Chemical Society* **2005,** *127* (39), 13466-7.
80. Suen, W. C.; Zhang, N.; Xiao, L.; Madison, V.; Zaks, A., Improved activity and thermostability of Candida antarctica lipase B by DNA family shuffling. *Protein Eng Des Sel* **2004,** *17* (2), 133-40.
81. Jung, S.; Park, S., Improving the expression yield of Candida antarctica lipase B in Escherichia coli by mutagenesis. *Biotechnol Lett* **2008,** *30* (4), 717-22.

82. Liu, D.; Schmid, R. D.; Rusnak, M., Functional expression of Candida antarctica lipase B in the Escherichia coli cytoplasm--a screening system for a frequently used biocatalyst. *Appl Microbiol Biotechnol* **2006,** *72* (5), 1024-32.
83. Ujiie, A.; Nakano, H.; Iwasaki, Y., Extracellular production of Pseudozyma (Candida) antarctica lipase B with genuine primary sequence in recombinant Escherichia coli. *J Biosci Bioeng* **2016,** *121* (3), 303-9.
84. Burdette, R. A.; Quinn, D. M., Interfacial reaction dynamics and acyl-enzyme mechanism for lipoprotein lipase-catalyzed hydrolysis of lipid p-nitrophenyl esters. *The Journal of biological chemistry* **1986,** *261* (26), 12016-21.
85. Cansu Ulker, N. G., Yuksel Guvenilir, Immobilization of candida antarctica lipase B (CALB) on surface-modified rice busk ashes (RHA) via physical adsorption and cross-linking methods. *Biocatal. Biotransform* **2016,** *34* (4), 172-180.
86. Zhang, N.; Suen, W. C.; Windsor, W.; Xiao, L.; Madison, V.; Zaks, A., Improving tolerance of Candida antarctica lipase B towards irreversible thermal inactivation through directed evolution. *Protein engineering* **2003,** *16* (8), 599-605.
87. Ashcroft, A. E.; Lago, H.; Macedo, J. M.; Horn, W. T.; Stonehouse, N. J.; Stockley, P. G., Engineering thermal stability in RNA phage capsids via disulphide bonds. *J Nanosci Nanotechnol* **2005,** *5* (12), 2034-41.
88. Bundy, B. C.; Swartz, J. R., Efficient disulfide bond formation in virus-like particles. *Journal of biotechnology* **2011,** *154* (4), 230-9.
89. Jewett, M. C.; Swartz, J. R., Rapid expression and purification of 100 nmol quantities of active protein using cell-free protein synthesis. *Biotechnology progress* **2004,** *20* (1), 102-9.
90. Abramoff, M. D., Magelhaes, P. J., Ram, S. J, Image processing with ImageJ. *Biophoton Int.* **2004,** *11*, 36-42.
91. Kavlock, R. J.; Daston, G. P.; DeRosa, C.; Fenner-Crisp, P.; Gray, L. E.; Kaattari, S.; Lucier, G.; Luster, M.; Mac, M. J.; Maczka, C., Research needs for the risk assessment of health and environmental effects of endocrine disruptors: a report of the US EPA-sponsored workshop. *Environmental health perspectives* **1996,** *104* (Suppl 4), 715.
92. Vogel, J. M., Perils of paradigm: Complexity, policy design, and the Endocrine Disruptor Screening Program. *Environmental Health* **2005,** *4* (1), 1.
93. De Coster, S.; van Larebeke, N., Endocrine-disrupting chemicals: associated disorders and mechanisms of action. *Journal of environmental and public health* **2012,** *2012*.
94. Scognamiglio, V.; Antonacci, A.; Patrolecco, L.; Lambreva, M. D.; Litescu, S. C.; Ghuge, S. A.; Rea, G., Analytical tools monitoring endocrine disrupting chemicals. *TrAC Trends in Analytical Chemistry* **2016,** *80*, 555-567.
95. Attina, T. M.; Hauser, R.; Sathyanarayana, S.; Hunt, P. A.; Bourguignon, J.-P.; Myers, J. P.; DiGangi, J.; Zoeller, R. T.; Trasande, L., Exposure to endocrine-disrupting chemicals in the USA: a population-based disease burden and cost analysis. *The Lancet Diabetes & Endocrinology* **2016,** *4* (12), 996-1003.
96. Teixeira, D.; Pestana, D.; Santos, C.; Correia-Sá, L.; Marques, C.; Norberto, S.; Meireles, M.; Faria, A.; Silva, R.; Faria, G., Inflammatory and cardiometabolic risk on obesity: role of environmental xenoestrogens. *The Journal of Clinical Endocrinology & Metabolism* **2015,** *100* (5), 1792-1801.
97. Watson, C. S.; Hu, G.; Paulucci-Holthauzen, A. A., Rapid actions of xenoestrogens disrupt normal estrogenic signaling. *Steroids* **2014,** *81*, 36-42.

98. Vilahur, N.; Fernández, M. F.; Bustamante, M.; Ramos, R.; Forns, J.; Ballester, F.; Murcia, M.; Riaño, I.; Ibarluzea, J.; Olea, N., In utero exposure to mixtures of xenoestrogens and child neuropsychological development. *Environmental research* **2014,** *134*, 98-104.
99. Vilahur, N.; Bustamante, M.; Byun, H.-M.; Fernandez, M. F.; Santa Marina, L.; Basterrechea, M.; Ballester, F.; Murcia, M.; Tardón, A.; Fernández-Somoano, A., Prenatal exposure to mixtures of xenoestrogens and repetitive element DNA methylation changes in human placenta. *Environment international* **2014,** *71*, 81-87.
100. Richter, C. A.; Birnbaum, L. S.; Farabollini, F.; Newbold, R. R.; Rubin, B. S.; Talsness, C. E.; Vandenbergh, J. G.; Walser-Kuntz, D. R.; vom Saal, F. S., In vivo effects of bisphenol A in laboratory rodent studies. *Reproductive toxicology* **2007,** *24* (2), 199-224.
101. Chapin, R. E.; Adams, J.; Boekelheide, K.; Gray, L. E.; Hayward, S. W.; Lees, P. S.; McIntyre, B. S.; Portier, K. M.; Schnorr, T. M.; Selevan, S. G., NTP‐CERHR expert panel report on the reproductive and developmental toxicity of bisphenol A. *Birth Defects Research Part B: Developmental and Reproductive Toxicology* **2008,** *83* (3), 157-395.
102. Viñas, R.; Watson, C. S., Mixtures of xenoestrogens disrupt estradiol-induced non-genomic signaling and downstream functions in pituitary cells. *Environmental Health* **2013,** *12* (1), 1.
103. Braun, J. M.; Kalkbrenner, A. E.; Calafat, A. M.; Yolton, K.; Ye, X.; Dietrich, K. N.; Lanphear, B. P., Impact of early-life bisphenol A exposure on behavior and executive function in children. *Pediatrics* **2011,** *128* (5), 873-882.
104. Bhandari, R. K.; Deem, S. L.; Holliday, D. K.; Jandegian, C. M.; Kassotis, C. D.; Nagel, S. C.; Tillitt, D. E.; vom Saal, F. S.; Rosenfeld, C. S., Effects of the environmental estrogenic contaminants bisphenol A and 17α-ethinyl estradiol on sexual development and adult behaviors in aquatic wildlife species. *General and comparative endocrinology* **2015,** *214*, 195-219.
105. Wetherill, Y. B.; Akingbemi, B. T.; Kanno, J.; McLachlan, J. A.; Nadal, A.; Sonnenschein, C.; Watson, C. S.; Zoeller, R. T.; Belcher, S. M., In vitro molecular mechanisms of bisphenol A action. *Reproductive toxicology* **2007,** *24* (2), 178-198.
106. vom Saal, F. S.; Welshons, W. V., Evidence that bisphenol A (BPA) can be accurately measured without contamination in human serum and urine, and that BPA causes numerous hazards from multiple routes of exposure. *Molecular and cellular endocrinology* **2014,** *398* (1), 101-113.
107. Kim, B. K.; Li, J.; Im, J.-E.; Ahn, K.-S.; San Park, T.; Cho, S. I.; Kim, Y.-R.; Lee, W.-Y., Impedometric estrogen biosensor based on estrogen receptor alpha-immobilized gold electrode. *Journal of Electroanalytical Chemistry* **2012,** *671*, 106-111.
108. Yildirim, N.; Long, F.; Gao, C.; He, M.; Shi, H.-C.; Gu, A. Z., Aptamer-based optical biosensor for rapid and sensitive detection of 17β-estradiol in water samples. *Environmental science & technology* **2012,** *46* (6), 3288-3294.
109. Ye, X.; Kuklenyik, Z.; Needham, L. L.; Calafat, A. M., Automated on-line column-switching HPLC-MS/MS method with peak focusing for the determination of nine environmental phenols in urine. *Analytical chemistry* **2005,** *77* (16), 5407-5413.
110. Covaci, A.; Den Hond, E.; Geens, T.; Govarts, E.; Koppen, G.; Frederiksen, H.; Knudsen, L. E.; Mørck, T. A.; Gutleb, A. C.; Guignard, C., Urinary BPA measurements in children and mothers from six European member states: overall results and determinants of exposure. *Environmental research* **2015,** *141*, 77-85.
111. Tomaszewski, M.; White, C.; Patel, P.; Masca, N.; Damani, R.; Hepworth, J.; Samani, N. J.; Gupta, P.; Madira, W.; Stanley, A., High rates of non-adherence to antihypertensive treatment

revealed by high-performance liquid chromatography-tandem mass spectrometry (HP LC-MS/MS) urine analysis. *Heart* **2014**, heartjnl-2013-305063.
112. Leusch, F. D.; De Jager, C.; Levi, Y.; Lim, R.; Puijker, L.; Sacher, F.; Tremblay, L. A.; Wilson, V. S.; Chapman, H. F., Comparison of five in vitro bioassays to measure estrogenic activity in environmental waters. *Environmental science & technology* **2010,** *44* (10), 3853-3860.
113. Gierach, I.; Li, J.; Wu, W.-Y.; Grover, G. J.; Wood, D. W., Bacterial biosensors for screening isoform-selective ligands for human thyroid receptors α-1 and β-1. *FEBS open bio* **2012,** *2*, 247-253.
114. Organization, W. H., WHO model list of essential medicines: 16th list (updated) March 2010. **2010**.
115. Johansen, L. M.; Brannan, J. M.; Delos, S. E.; Shoemaker, C. J.; Stossel, A.; Lear, C.; Hoffstrom, B. G.; DeWald, L. E.; Schornberg, K. L.; Scully, C., FDA-approved selective estrogen receptor modulators inhibit Ebola virus infection. *Science translational medicine* **2013,** *5* (190), 190ra79-190ra79.
116. Moens, S. J. B.; Schnitzler, G. R.; Nickerson, M.; Guo, H.; Ueda, K.; Lu, Q.; Aronovitz, M. J.; Nickerson, H.; Baur, W. E.; Hansen, U., Rapid estrogen receptor signaling is essential for the protective effects of estrogen against vascular injury. *Circulation* **2012,** *126* (16), 1993-2004.
117. Salehi, A. S.; Shakalli Tang, M. J.; Smith, M. T.; Hunt, J. M.; Law, R. A.; Wood, D. W.; Bundy, B. C., Cell-Free Protein Synthesis Approach to Biosensing hTRβ-Specific Endocrine Disruptors. *Analytical Chemistry* **2017,** *89* (6), 3395-3401.
118. Gierach, I.; Shapero, K.; Eyster, T. W.; Wood, D. W., Bacterial biosensors for evaluating potential impacts of estrogenic endocrine disrupting compounds in multiple species. *Environ. Toxicol.* **2013,** *28* (4), 179-189.
119. Vandenberg, L. N.; Prins, G. S., Clarity in the face of confusion: new studies tip the scales on bisphenol A (BPA). *Andrology* **2016,** *4* (4), 561-4.
120. Li, X.; Franke, A. A., Improvement of bisphenol A quantitation from urine by LCMS. *Anal Bioanal Chem* **2015,** *407* (13), 3869-74.
121. Shaykhutdinov, R., MacInnis, G., Dowlatabadi, R., Weljie, A., Vogel, H., Quantitative analysis of metabolite concentrations in human urine samples using 13C{1H} NMR spectroscopy. *Metabolomics* **2009,** *5* (3), 307-317.
122. Taylor, A. J.; Vadgama, P., Analytical reviews in clinical biochemistry: the estimation of urea. *Ann Clin Biochem* **1992,** *29 (Pt 3)*, 245-64.
123. Putnam, D. F. *Composition and concentrative properties of human urine*; CF-1802; NASA: Washington, DC, 1971.
124. Salehi, A. S.; Shakalli Tang, M. J.; Smith, M. T.; Hunt, J. M.; Law, R. A.; Wood, D. W.; Bundy, B. C., Cell-Free Protein Synthesis Approach to Biosensing hTRbeta-Specific Endocrine Disruptors. *Analytical chemistry* **2017,** *89* (6), 3395-3401.
125. Blank, A.; Dekker, C. A., Ribonucleases of human serum, urine, cerebrospinal fluid, and leukocytes. Activity staining following electrophoresis in sodium dodecyl sulfate-polyacrylamide gels. *Biochemistry* **1981,** *20* (8), 2261-7.
126. Iwama, M.; Kunihiro, M.; Ohgi, K.; Irie, M., Purification and properties of human urine ribonucleases. *J Biochem* **1981,** *89* (4), 1005-16.
127. Landre, J. B.; Hewett, P. W.; Olivot, J. M.; Friedl, P.; Ko, Y.; Sachinidis, A.; Moenner, M., Human endothelial cells selectively express large amounts of pancreatic-type ribonuclease (RNase 1). *J Cell Biochem* **2002,** *86* (3), 540-52.

128. Bourgeois, S.; Gernet, M.; Pradeau, D.; Andremont, A.; Fattal, E., Evaluation of critical formulation parameters influencing the bioactivity of β-lactamases entrapped in pectin beads. *Int. J. Pharm.* **2006,** *324* (1), 2-9.
129. O'Connell, M. A., Belanger, B. A., Haaland, P. D., Calibration and assay development using the four-parameter logistic model. *Chemometrics and Intelligent Laboratory Systems* **1993,** *20*, 97-114.
130. Gierach, I.; Shapero, K.; Eyster, T. W.; Wood, D. W., Bacterial biosensors for evaluating potential impacts of estrogenic endocrine disrupting compounds in multiple species. *Environ Toxicol* **2013,** *28* (4), 179-89.
131. Zhang, J. H.; Chung, T. D.; Oldenburg, K. R., A Simple Statistical Parameter for Use in Evaluation and Validation of High Throughput Screening Assays. *J Biomol Screen* **1999,** *4* (2), 67-73.
132. Vareiro, M. M.; Liu, J.; Knoll, W.; Zak, K.; Williams, D.; Jenkins, A. T., Surface plasmon fluorescence measurements of human chorionic gonadotrophin: role of antibody orientation in obtaining enhanced sensitivity and limit of detection. *Analytical chemistry* **2005,** *77* (8), 2426-31.
133. FDA, U. S. Information on Biosimilars. https://www.fda.gov/Drugs/DevelopmentApprovalProcess/HowDrugsareDevelopedandApproved/ApprovalApplications/TherapeuticBiologicApplications/Biosimilars/.
134. Markets, M. a. Biosimilars Market by Product (Recombinant Non-glycosylated Proteins (Insulin, rHGH, Interferon), glycosylated (mAb, EPO), Peptides (Glucagon, Calcitonin)), Manufacturing (In-House, CMO), Application (Oncology, Blood Disorders) - Global Forecast to 2021. http://www.marketsandmarkets.com/Market-Reports/biosimilars-40.html (accessed April 26th).
135. Cornes, P., The economic pressures for biosimilar drug use in cancer medicine. *Target Oncol* **2012,** *7 Suppl 1*, S57-67.
136. Majidzadeh, A. K.; Mahboudi, F.; Hemayatkar, M.; Davami, F.; Barkhordary, F.; Adeli, A.; Soleimani, M.; Davoudi, N.; Khalaj, V., Human Tissue Plasminogen Activator Expression in Escherichia coli using Cytoplasmic and Periplasmic Cumulative Power. *Avicenna J Med Biotechnol* **2010,** *2* (3), 131-6.
137. Qiu, J.; Swartz, J. R.; Georgiou, G., Expression of active human tissue-type plasminogen activator in Escherichia coli. *Applied and environmental microbiology* **1998,** *64* (12), 4891-6.
138. Lee, H. J., Im, H., Soluble expression and purification of human tissue-type plasminogen activator protease domain. *Bull Korean Chem Soc* **2010,** *31* (9), 2607-2612.
139. Fathi-Roudsari, M.; Akhavian-Tehrani, A.; Maghsoudi, N., Comparison of Three Escherichia coli Strains in Recombinant Production of Reteplase. *Avicenna J Med Biotechnol* **2016,** *8* (1), 16-22.
140. Gravanis, I., and Tsirka, S. E., tPA as a therapeutic target in stroke. *Expert Opin Ther Targets* **2008,** *12* (2).
141. Fonarow, G. C.; Smith, E. E.; Reeves, M. J.; Pan, W.; Olson, D.; Hernandez, A. F.; Peterson, E. D.; Schwamm, L. H.; Get With The Guidelines Steering, C.; Hospitals, Hospital-level variation in mortality and rehospitalization for medicare beneficiaries with acute ischemic stroke. *Stroke* **2011,** *42* (1), 159-66.
142. Pennica, D.; Holmes, W. E.; Kohr, W. J.; Harkins, R. N.; Vehar, G. A.; Ward, C. A.; Bennett, W. F.; Yelverton, E.; Seeburg, P. H.; Heyneker, H. L.; Goeddel, D. V.; Collen, D.,

Cloning and expression of human tissue-type plasminogen activator cDNA in E. coli. *Nature* **1983,** *301* (5897), 214-21.
143. Furlong, A. M.; Thomsen, D. R.; Marotti, K. R.; Post, L. E.; Sharma, S. K., Active human tissue plasminogen activator secreted from insect cells using a baculovirus vector. *Biotechnol Appl Biochem* **1988,** *10* (5), 454-64.
144. Martegani, E.; Forlani, N.; Mauri, I.; Porro, D.; Schleuning, W. D.; Alberghina, L., Expression of high levels of human tissue plasminogen activator in yeast under the control of an inducible GAL promoter. *Appl Microbiol Biotechnol* **1992,** *37* (5), 604-8.
145. Steiner, H.; Pohl, G.; Gunne, H.; Hellers, M.; Elhammer, A.; Hansson, L., Human tissue-type plasminogen activator synthesized by using a baculovirus vector in insect cells compared with human plasminogen activator produced in mouse cells. *Gene* **1988,** *73* (2), 449-57.
146. Chen, J.; Song, J. L.; Zhang, S.; Wang, Y.; Cui, D. F.; Wang, C. C., Chaperone activity of DsbC. *The Journal of biological chemistry* **1999,** *274* (28), 19601-5.
147. Maskos, K.; Huber-Wunderlich, M.; Glockshuber, R., DsbA and DsbC-catalyzed oxidative folding of proteins with complex disulfide bridge patterns in vitro and in vivo. *Journal of molecular biology* **2003,** *325* (3), 495-513.
148. Zhang, Z.; Li, Z. H.; Wang, F.; Fang, M.; Yin, C. C.; Zhou, Z. Y.; Lin, Q.; Huang, H. L., Overexpression of DsbC and DsbG markedly improves soluble and functional expression of single-chain Fv antibodies in Escherichia coli. *Protein Expr Purif* **2002,** *26* (2), 218-28.
149. Pohl, G.; Kallstrom, M.; Bergsdorf, N.; Wallen, P.; Jornvall, H., Tissue plasminogen activator: peptide analyses confirm an indirectly derived amino acid sequence, identify the active site serine residue, establish glycosylation sites, and localize variant differences. *Biochemistry* **1984,** *23* (16), 3701-7.
150. Wallen, P.; Pohl, G.; Bergsdorf, N.; Ranby, M.; Ny, T.; Jornvall, H., Purification and characterization of a melanoma cell plasminogen activator. *European journal of biochemistry / FEBS* **1983,** *132* (3), 681-6.
151. Rajapakse, S.; Ogiwara, K.; Takano, N.; Moriyama, A.; Takahashi, T., Biochemical characterization of human kallikrein 8 and its possible involvement in the degradation of extracellular matrix proteins. *FEBS letters* **2005,** *579* (30), 6879-84.
152. Rijken, D. C.; Hoylaerts, M.; Collen, D., Fibrinolytic properties of one-chain and two-chain human extrinsic (tissue-type) plasminogen activator. *The Journal of biological chemistry* **1982,** *257* (6), 2920-5.
153. Strongin, A. Y.; Gorodetsky, D. I.; Stepanov, V. M., The study of Escherichia coli proteases. Intracellular serine protease of E. coli-an analogue of bacillus proteases. *J Gen Microbiol* **1979,** *110* (2), 443-51.
154. Rodier, M.; Prigent-Tessier, A.; Bejot, Y.; Jacquin, A.; Mossiat, C.; Marie, C.; Garnier, P., Exogenous t-PA administration increases hippocampal mature BDNF levels. plasmin- or NMDA-dependent mechanism? *PloS one* **2014,** *9* (3), e92416.
155. Geng, Y.; Wang, S.; Qi, Q., Expression of active recombinant human tissue-type plasminogen activator by using in vivo polyhydroxybutyrate granule display. *Applied and environmental microbiology* **2010,** *76* (21), 7226-30.
156. Wittwer, A. J.; Howard, S. C.; Carr, L. S.; Harakas, N. K.; Feder, J.; Parekh, R. B.; Rudd, P. M.; Dwek, R. A.; Rademacher, T. W., Effects of N-glycosylation on in vitro activity of Bowes melanoma and human colon fibroblast derived tissue plasminogen activator. *Biochemistry* **1989,** *28* (19), 7662-9.

157. Einarsson, M.; Brandt, J.; Kaplan, L., Large-scale purification of human tissue-type plasminogen activator using monoclonal antibodies. *Biochimica et biophysica acta* **1985,** *830* (1), 1-10.
158. Xu, W.; Ellington, A. D., Anti-peptide aptamers recognize amino acid sequence and bind a protein epitope. *Proceedings of the National Academy of Sciences of the United States of America* **1996,** *93* (15), 7475-80.

APPENDIX A. SUPPLEMENTARY MATERIAL FOR CHAPTER 2

This supplementary material contains information about expression level of the guest enzyme and capsid, RNA aptamer design, and purification process of the capsid.

A.1 RNA Aptamer Transcription

The infectious bacteriophage Qβ encapsulates single-stranded RNA via a strong affinity between a hairpin loop on the RNA and residues on the interior surface of the Qβ coat protein.[65] This interaction is conserved even when recombinant Qβ coat protein is expressed to form virus-like particles.[64] In addition to the hairpin loop, an RNA aptamer was developed to possess a high affinity to bind specifically to an arginine-rich peptide (Rev) from HIV-1.[158] In order to make an RNA aptamer, Rev recognition sequence was inserted just upstream of the Qβ coat protein region, and the hairpin loop forming sequence was inserted just downstream of the Qβ coat protein region (Figure A-1). The polymerase chain reaction (PCR) amplified the whole linear

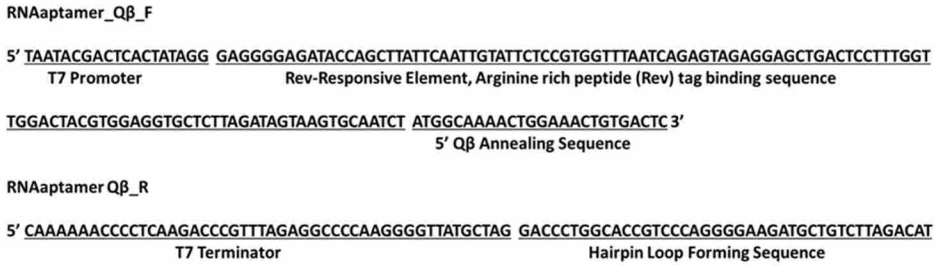

Figure A-1 Primers for the RNA aptamer design Qβ capsid DNA sequence was used as a template for the RNA aptamer. The upstream of the capsid sequence possesses Rev tag binding sequence, while the hairpin loop sequence was fused to the downstream of the capsid sequence. The melting temperature of both primers were 56˚C and 54.9˚C for RNAaptamer_Qβ_F and RNAaptamer Qβ_R, respectively. Only 3 μL of 10 μM of both primers were added to the PCR reaction to avoid primer dimer formation while 1 μL of the DNA template (pY71-Qβ) was added to the reaction.

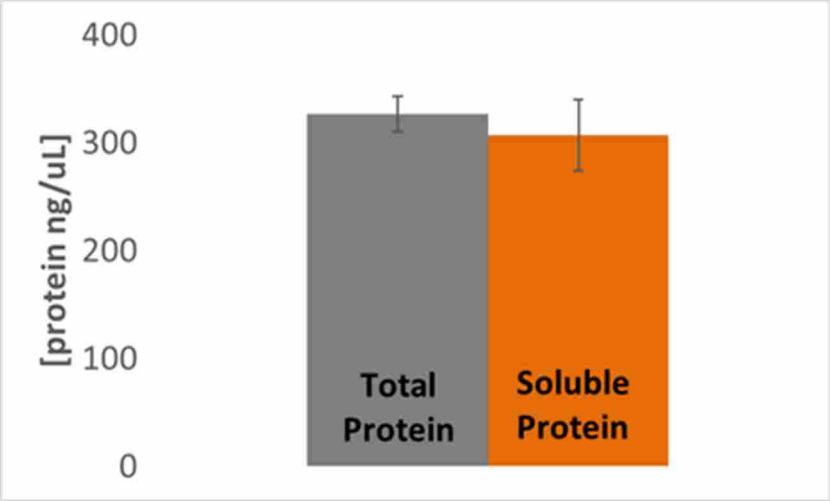

Figure A-2 Rev-CalB CFPS expression Rev-CalB was expressed in the CFPS where overexpressed GroEL/ES and a buffer containing mixture of glutathione oxidized (GSSG) and reduced (GSH). 70 μL CFPS reaction resulted in an average 306.8 ng/μL of the enzyme production. Higher than 93% of the enzyme produced were soluble.

DNA containing T7 promoter, Rev recognition, Qβ coat protein, the hairpin loop, and T7 terminator sequence. T7 RNA polymerase transcribed the linear DNA. Isopropanol precipitation method purified a pure RNA aptamer, and the RNA was reconstituted with RNAse free water until the usage.

A.2 CalB Optimization

To optimize soluble CalB production, bacterial chaperonine protein (GroEL/ES) and a glutathione buffer mix (5 mM of GSSG and GSH) were added to the CFPS reaction. Total reaction time was five hours at 30˚C to reduce the formation of inclusion bodies and enhance correct folding of the protein (Figure A-2).

A.3 Capsid Protein Production with a Buffer Mix Containing GSSG and GSH

Qβ capsid production was optimized without a buffer containing GSSG and GSH. The capsid can not be produced without the glutathione buffer mix for CalB encapsulation because the buffer was transferred with the enzyme from “step 1”. Upon transferring the CFPS reaction

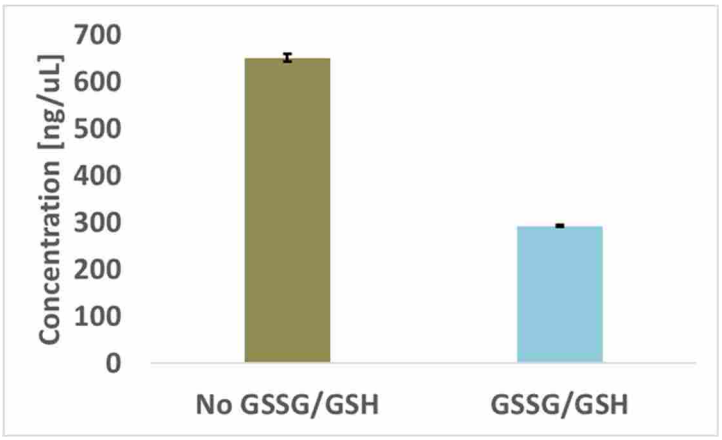

Figure A-3 Glutathion mixture affects CFPS of Qβ coat protein Expression of Qβ coat protein in the CFPS is decreased by a factor of two upon introducing the mixture of glutathione oxidized (GSSG) and reduced (GSH).

of CalB to the capsid CFPS reaction, the total capsid production level dropped due to the glutathione buffer (Figure A-3).

A.4 Guest Enzyme Containing Capsid Purification Process

A hexa-Histidine (His_{6x}) tag fused capsid was purified by a His column (Figure A-4). Not all the capsids bound to the nickel affinity column, because some capsids are missing the His_{6x}-

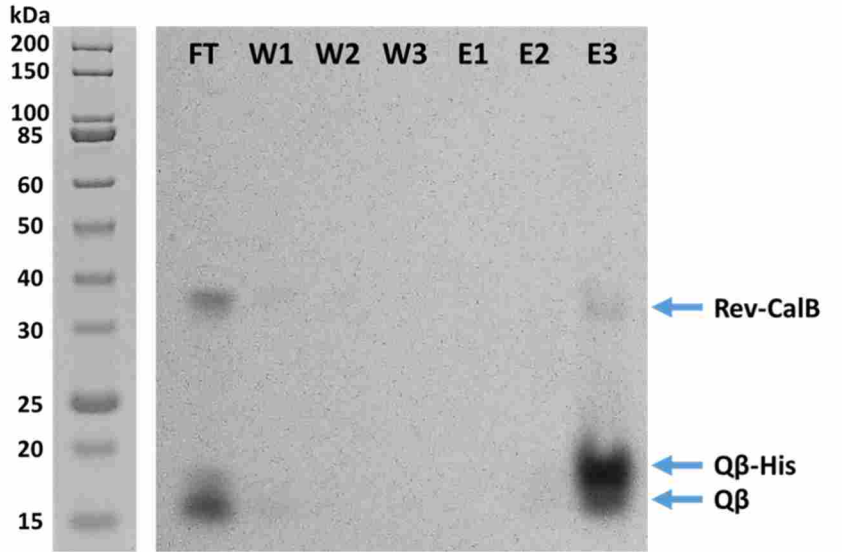

Figure A-4 Rev-CalB Containing Qβ Capsid Purification SDS-PAGE gel was exposed to an autoradiography film to show where both the enzyme and the capsid were eluded. Almost all capsid and enzyme complex eluted out at 500 mM imidazole containing buffer. The capsid without the Qβ-His did not bind to the nickel affinity column so was the non-encapsulated Rev-CalB.

tag, or have a lower number of tags. Most of the Rev-CalB enzymes (non-encapsulated) were found in the flow through fraction. Almost all capsids containing Rev-CalB were eluted out with a buffer containing 500 mM imidazole.